Functionalized osteoarthritis targeting peptides for MRI, lubricant and regenerative medicine

Chin-Yu Lin
China Medical University
Yung-Li Wang
China Medical University
Yi-Hsuan Chi
Academia Sinica
Long Yi Chan
China Medical University
Kuan-Wen Chen
GGA Corporation
Horng-Chaung Hsu
China Medical University Hospital
Dennis W Hwang
Academia Sinica
Han-Chung Wu
Academia Sinica
Shih-Chieh Hung (hung3340@gmail.com)
Institute of New Drug Development, China Medical University

Article

Keywords: osteoarthritis, magnetic resonance imaging, regenerative medicine

Posted Date: November 6th, 2020

DOI: https://doi.org/10.21203/rs.3.rs-87673/v1

Functionalized osteoarthritis targeting peptides for MRI, lubricant and regenerative medicine

Short title*: *Osteoarthritis targeting peptides

Chin-Yu Lin[1,#], Yung-Li Wang[1,#], Yi-Hsuan Chi[2], Long Yi Chan[1], Guan-Wen Chen[3], Horng-Chaung Hsu[4, 5], Dennis W Hwang[7], Han-Chung Wu[2]*, Shih-Chieh Hung[1, 5, 6]*

[1]Institute of New Drug Development, School of Medicine, China Medical University, Taichung, 40402, Taiwan
[2]Institute of Cellular and Organismic Biology, Academia Sinica, Taipei 11529, Taiwan
[3]Molecular Science Center, GGA Corporation, Taipei 11494, Taiwan
[4]Department of Medicine, School of Medicine, China Medical University, Taichung, 40402, Taiwan
[5]Department of Orthopaedics, China Medical University Hospital, Taichung, 40447, Taiwan
[6]Integrative Stem Cell Center, China Medical University Hospital, Taichung, 40447, Taiwan
[7]Institute of Biomedical Sciences, Academia Sinica, Taipei 11529, Taiwan

[#]Equal contribution

*Correspondence should be addressed to Shih-Chieh Hung (hung3340@gmail.com) and Han-Chung Wu (hcw0928@gate.sinica.edu.tw)

Shih-Chieh Hung, M.D. Ph.D., Distinguished Professor & Director, Institute of New Drug Development, China Medical University, No.91 Hsueh-Shih Road, North District, Taichung, 40402, Taiwan.
Tel: (+886)4-2205-2121#7728; Fax: (+886)4-2233-3922; E-mail: hung3340@gmail.com

Abstract

Despite the efforts made for osteoarthritis (OA) treatment, the results are limited and can be improved by enhancing the OA homing strategy. Here, we used a phage display system to identify OA-targeting peptides, and combined them with magnetic resonance imaging detection reagents to expand their application to early OA diagnosis in rat and swine models. OA-targeting peptides showed better static and kinetic friction characteristics than scrambled peptides, when conjugated with hyaluronic acid for rheological lubrication studies using human OA specimens. Furthermore, mesenchymal stem cells, through CD44 binding to hyaluronic acid conjugated with OA-targeting peptides, showed better capacity for OA homing and repair than those conjugated with scrambled peptides. Protein–peptide docking revealed WXPXW as the consensus binding motifs that bind to collagen XII, a protein exclusively expressed in human and animal OA models. These results suggest the potential of OA-targeting peptides to promote diagnosis, treatment, and regenerative medicine for OA.

Keywords: Osteoarthritis, Targeting peptide, Therapeutics, Diagnostics, Joint lubricant. Collagen XII

Because articular cartilage lacks the capacity for self-repair, incidences of osteoarthritis (OA) are increasing, especially for those older than 60 years of age[1]. Medication with anti-inflammatory drugs, intra-articular injection with lubricating supplements, and surgeries including microfracture and mosaicplasty remain the current modalities for OA treatment, only alleviating symptoms. There are no disease-modifying agents for OA. Cell-based therapy using autologous chondrocyte implantation was only effective in treating focal articular cartilage defects[2]. Transplantation of stem cells or progenitor cells has now emerged as an alternative for chondrocytes in the treatment of OA and osteochondral defects, especially for large lesions[3].

Mesenchymal stem cells (MSCs), with capacities of self-renewal and multipotent differentiation, are not only used to repair mesenchymal tissues but also used in tissue engineering of cartilage and bone[4]. The long-term safety of intra-articular injection of MSCs has been demonstrated in 41 patients with knee OA[3]. Furthermore, the clinical efficacy and safety of MSC transplantation for OA treatment has been demonstrated in a meta-analysis with 11 eligible trials and 582 knee OA patients[5].

A two-year follow-up study regarding the efficacy of intra-articular injection of MSCs for the treatment of knee OA revealed potential concerns about the durability of clinical and structural outcomes in low- and intermediate-dose arms of treatment[6], suggesting the need for further studies. Intra-articular injection of MSCs with hyaluronic acid (HA) as a vehicle showed a superior effect than injection of HA alone for the treatment of OA induced by anterior cruciate ligament (ACL) transection[7]. This study and others[8] revealed that nonspecific binding of MSCs onto the synovium, meniscus, and ligamentous tissues, highlighted the importance of the development of methods for enhancing local delivery of cells to injured articular cartilage. However, there are few, if any, studies focusing on this. Magnetically labeled MSCs have been applied for articular cartilage

repair[9]. Although MSCs labeled with magnetic particles exhibit no deterioration in chondrogenic differentiation, there is concern about the uptake of iron by the tissues.

In the current study, we identified OA-targeting peptides through biopanning of a phage display peptide library with the use of human OA specimens. The OA-targeting peptides were further investigated for application in the delivery of diagnostic agents, lubrication supplements, and MSCs to articular surfaces in an enzyme-induced OA rat model and in an ACL-transection OA swine model.

Identification of OA-targeting peptides

Using a phage display peptide library, we probed the OA articular cartilage cut from the subchondral bone of knee joints from patients who received total knee joint replacement. The OA cartilage specimens were homogenized for acquiring tissue lysates or cut into square tissue pieces, 5 mm × 5 mm in size. Through five rounds of selection of phage-displayed peptides (biopanning) binding to tissue lysates and tissue pieces (Fig. S1), the titers of bound phages significantly increased up to 388-fold (Fig. S2a), and 864-fold (Fig. S2b), respectively. Phage clones collected from the fifth round of biopanning were further subjected to ELISA screening, and clones with high affinity to tissue lysates or pieces were chosen, sequenced, and aligned (Fig. S2c and S2d). Finally, we identified five groups of targeting phages sharing distinctive consensus motifs (Table S1). The binding abilities of selected phage clones were validated in the human chondrocyte cell line, hPi-GL[10], by immunocytofluorescent staining. All of the identified phage clones, labeled with M13-PE (antibody conjugated to fluorescent dye), bound to hPi-GL in a dose-dependent manner (Fig. S3a). Notably, C5-24 and C5-91 peptides showed specific and remarkable binding scenarios in hPi-GL (Fig. S3b). To examine phage clones specifically binding to OA cartilage (Fig. S4) rather

than to other soft tissues, such as the synovium and meniscus (Fig. S5), the human OA tissue sections were immunostained using horseradish peroxidase (HRP)-labeled phage clones, followed by semi-quantification of the deposited 3, 3 – diaminobenzidine (DAB) intensity (- to +++)[11]. Particularly, C5-24 and C5-91 peptides showed superior binding activity to cartilage, but no binding activity to the meniscus and synovium (Table S2). Moreover, C5-24 peptide exhibited the best specificity for targeting the territorial region of OA cartilage and was chosen for subsequent studies.

Intravital imaging of OA targeting

To demonstrate the OA-specific targeting activity of C5-24 peptides, rhodamine-labeled C5-24 peptides and scrambled peptides were separately injected into OA joints in a rat model for two-photon microscopy observation of fluorescence and second harmonic generation (SHG) signals. A scrambled peptide contains all the same amino acids as the original peptide but in new random order. Surface-rendered 3D reconstructed images and transversal composite images of cartilage showed sparse red dots randomly existing in the C5-24 peptide-injected control cartilage, scrambled peptide-injected control cartilage, and scrambled peptide-injected OA cartilage. Conversely, red dots were observed in the C5-24 peptide-injected OA cartilage. When probing type II collagen with SHG, red dots were localized in the SHG signal-free area (Fig. 1a), corresponding to the territorial region of OA cartilage. From the z-axial plane, it is determined that C5-24 peptides reached at least 50 μm in depth in the OA cartilage (Fig. 1a). In addition, the overall fluorescent peptide binding area (Fig. 1b) and binding intensity (Fig. 1c) in all slices were further calculated, showing a significant difference in C5-24 peptide targeting between OA and control cartilage.

These data demonstrate the distinguished recognition capability and specificity of C5-24 peptides for targeting the territorial regions of OA cartilage.

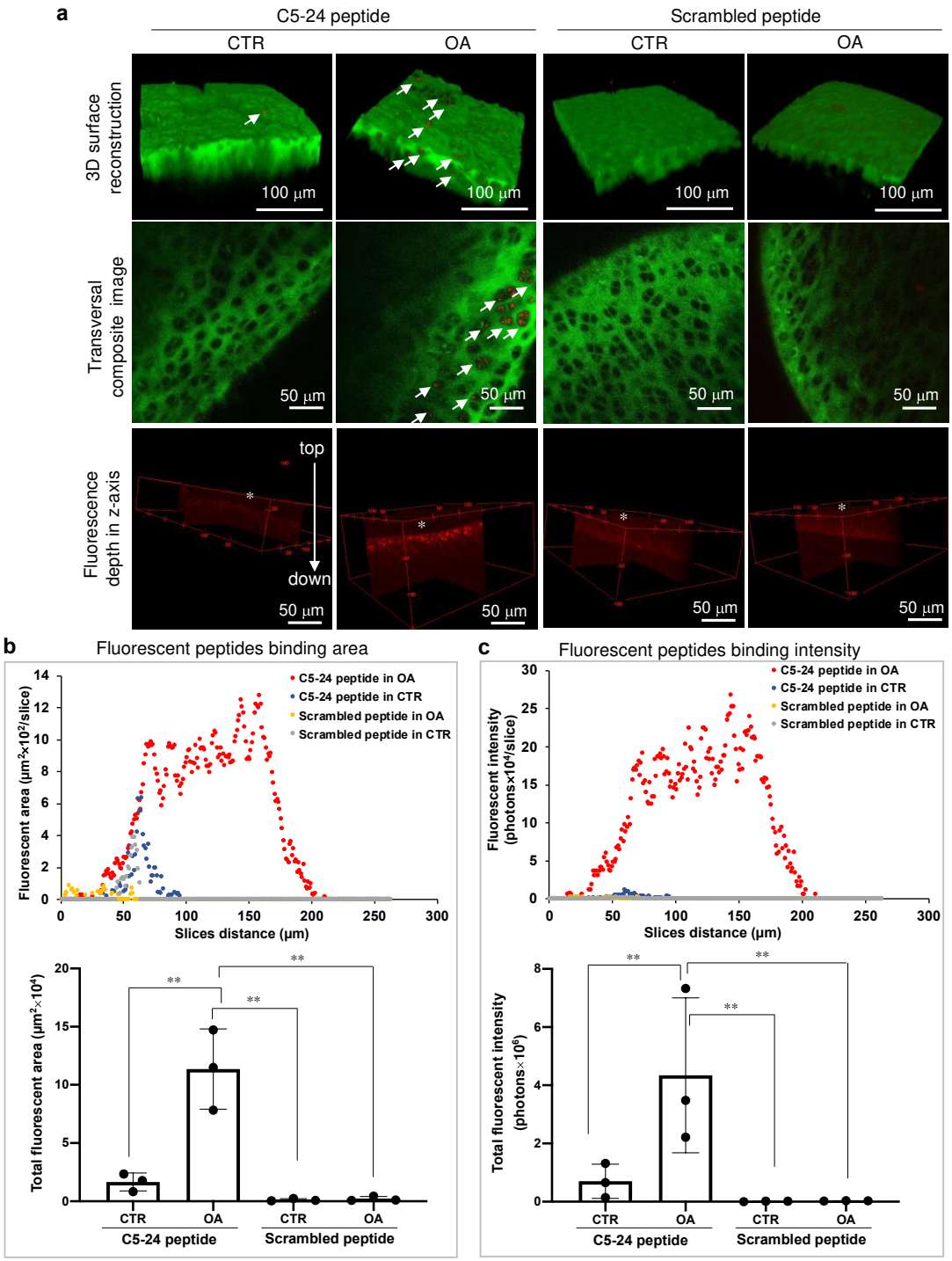

Fig. 1. Intravital imaging demonstrates the binding capability of C5-24 peptides to OA cartilage. The C5-24 peptides and scrambled peptides were fluorescently labeled and separately injected into rat knee joints pre-established without (CTR) or with OA. The whole joint capsules were removed at 24 h post-injection, and articular surfaces of the proximal tibiae were observed

under a two-photon microscope. **(a, upper and middle**, 3D and transversal images) Harmonic generation images of type II collagen are shown as green fluorescence. The peptides were labeled with rhodamine, showing red fluorescence (indicated by arrows). **(a, lower)** The fluorescent signals in all slices were reconstructed and the peptide penetration depths are shown in the x-z plane (cartilage surface is indicated by *). **(b)** Overall fluorescent peptide binding area in each slice (upper panel) and all groups (lower panel). **(c)** Overall fluorescent peptide binding intensity in each slice (upper panel) and all groups (lower panel). All images were reconstructed, merged and analyzed using ImageJ Fiji software. $^{**}p<0.01$

Application in early OA diagnosis

To demonstrate the applicability of OA-targeting peptides in the delivery of diagnostic agents for early diagnosis of OA, C5-24 and scrambled peptides were conjugated with superparamagnetic iron oxide (SPIO) (Fig. 2a). Fourier-transform infrared spectroscopy (FTIR) revealed increased N-H band/C-O stretch ratios, indicating successful installation of SPIO into C5-24 and scrambled peptides (Fig. 2b), which were intra-articularly injected into the OA joints of a rat model established by enzyme digestion[12]. Magnetic resonance imaging (MRI) of the OA knee joints without peptide-conjugated SPIO injection showed no difference compared to the sham control knee joints, revealing the challenge of MRI for early OA diagnosis when the articular cartilage is not severely denuded. Similarly, scrambled peptide-conjugated SPIO that did not bind to the OA cartilage, and the MRI signal reduction also failed to differentiate early OA from sham controls. Conversely, C5-24 peptide-conjugated SPIO bound to OA cartilage and caused MRI signal reduction in OA cartilage but not in healthy cartilage (Fig. 2c). To get one step closer to the clinical setting, the feasibility of C5-24 peptides-conjugated SPIO for early OA diagnosis was further confirmed in a large animal OA model established by ACL-transection in Lanyu minipigs. After 2 months of ACL-transection, the sham control knee joints either with or without receiving C5-24 peptides-conjugated SPIO or the OA knee joints without receiving C5-24 peptide-conjugated SPIO showed no difference in the T1- and T2-weighted MR images (Fig. 2d), indicating the difficulty in

using MRI for early OA diagnosis. However, the OA knee that received C5-24 peptide-conjugated SPIO showed enhanced signal reduction in T1- and T2-weighted MR images, demonstrating the sensitivity of C5-24 peptide-conjugated SPIO for early OA diagnosis. Taken together, these data suggest that imaging contrast agents, such as SPIO, when conjugated with C5-24 peptide, could be applied in early OA diagnosis in combination with the MR imaging system.

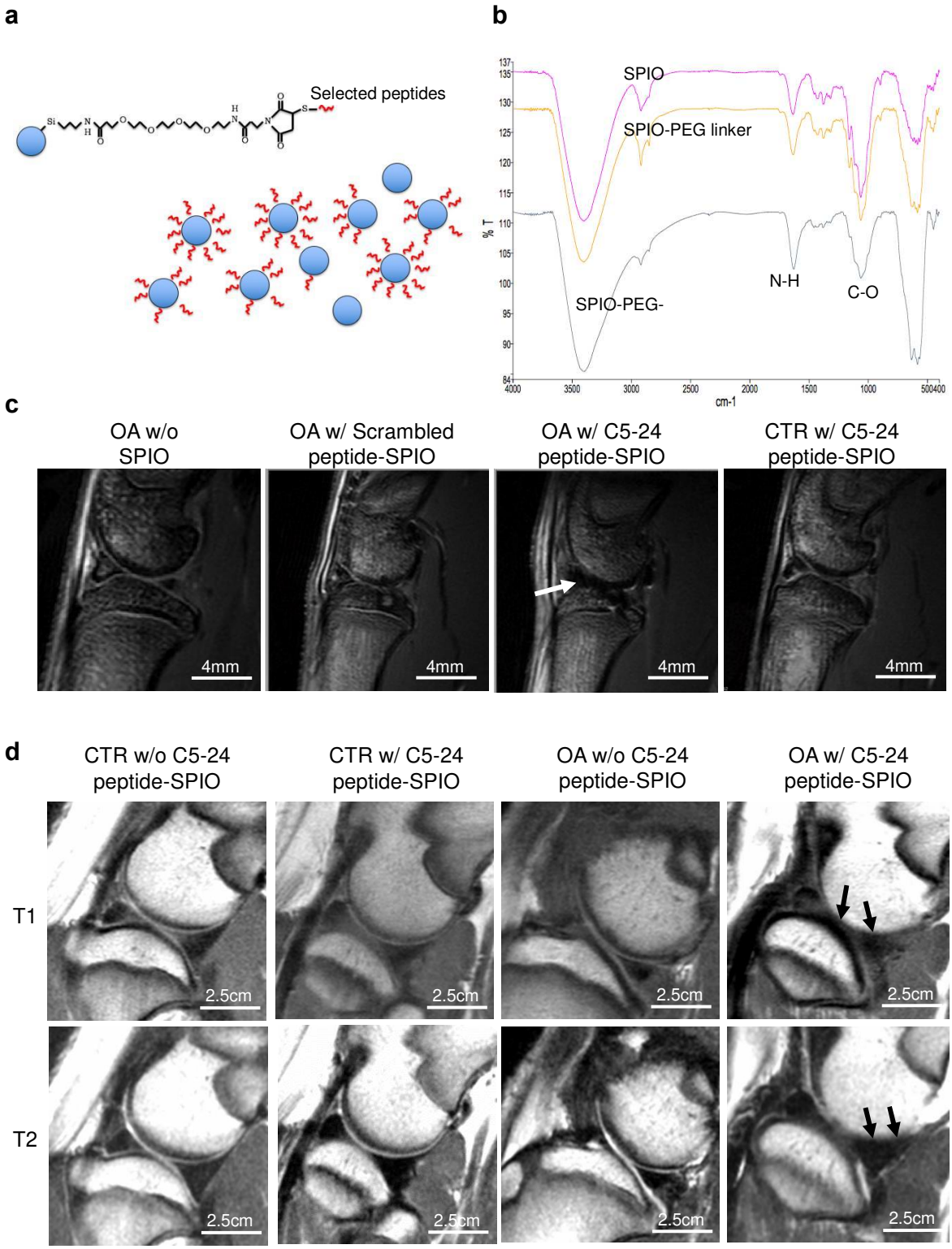

Fig. 2. Application of C5-24 peptides in early OA diagnosis. (a) Preparation of C5-24 peptides conjugated with SPIO for intraarticular injection. **(b)** FTIR analysis of SPIO-conjugated C5-24 peptides. **(c)** MR images of SPIO-conjugated C5-24 peptides bound to OA cartilage in a rat OA model. **(d)** MR images of SPIO-conjugated C5-24 peptides bound to OA cartilage in a Lanyu

minipig model. Binding of SPIO-conjugated C5-24 peptides to OA articular surface leads to signal intensity reduction (arrows).

Application in joint lubrication

To investigate the potential of C5-24 peptide to deliver HA into OA cartilage for lubrication, C5-24 peptides or scrambled peptides were conjugated with HA, referred to here as C5-24-HA and scrambled-HA, respectively (Fig. 3a). Methacrylation of HA-MA was measured by ^{1}H proton-NMR (Nuclear Magnetic Resonance) to be about 28.1%, which was used as intermediate product for subsequent C5-24 peptides (Fig. 3b) and scrambled peptides (Fig. S6) conjugation. The rheological lubrication properties, including static friction coefficient (μ_s) and kinetic friction coefficient (μ_k), were assessed using a rotational test protocol modified from a previous report[13], and compared among paired human OA cartilage cylinder discs (collected from 13 individuals) treated with non-modified HA, scrambled-HA, or C5-24-HA. The total friction coefficients for non-modified HA, scrambled-HA, and C5-24-HA in 1.2 s relaxation scenario were: 0.065, 0.073, and 0.044 in μ_s and 0.045, 0.052, and 0.034 in μ_k, respectively, with 32.3% and 24.4% reduction in C5-24-HA compared to non-modified HA; in 12 s relaxation scenario were: 0.072, 0.075, and 0.043 in μ_s and 0.045, 0.052, and 0.033 in μ_k, respectively, with 40.3% and 26.7% reduction in C5-24-HA compared to non-modified HA; in 120 s relaxation scenario were: 0.077, 0.079, and 0.044 in μ_s and 0.048, 0.055, and 0.034 in μ_k, respectively, with 42.9% and 29.2% reduction in C5-24-HA compared to non-modified HA; and in 1200 s relaxation scenario were: 0.094, 0.102, and 0.066 in μ_s and 0.060, 0.067, and 0.042 in μ_k, respectively, with 29.8% and 30% reduction in C5-24-HA compared to non-modified HA (Fig. 3c). Briefly, C5-24-HA showed statistically significant superior static and kinetic friction characteristics in comparison with non-modified HA and scrambled-HA in all relaxation stages, demonstrating superior lubrication. Moreover, C5-24-HA

exhibited better lubrication than non-modified HA and scrambled-HA in the rheological pre-condition stage (Fig. S7) and torque measurements (Fig. S8). Representative individual patient data

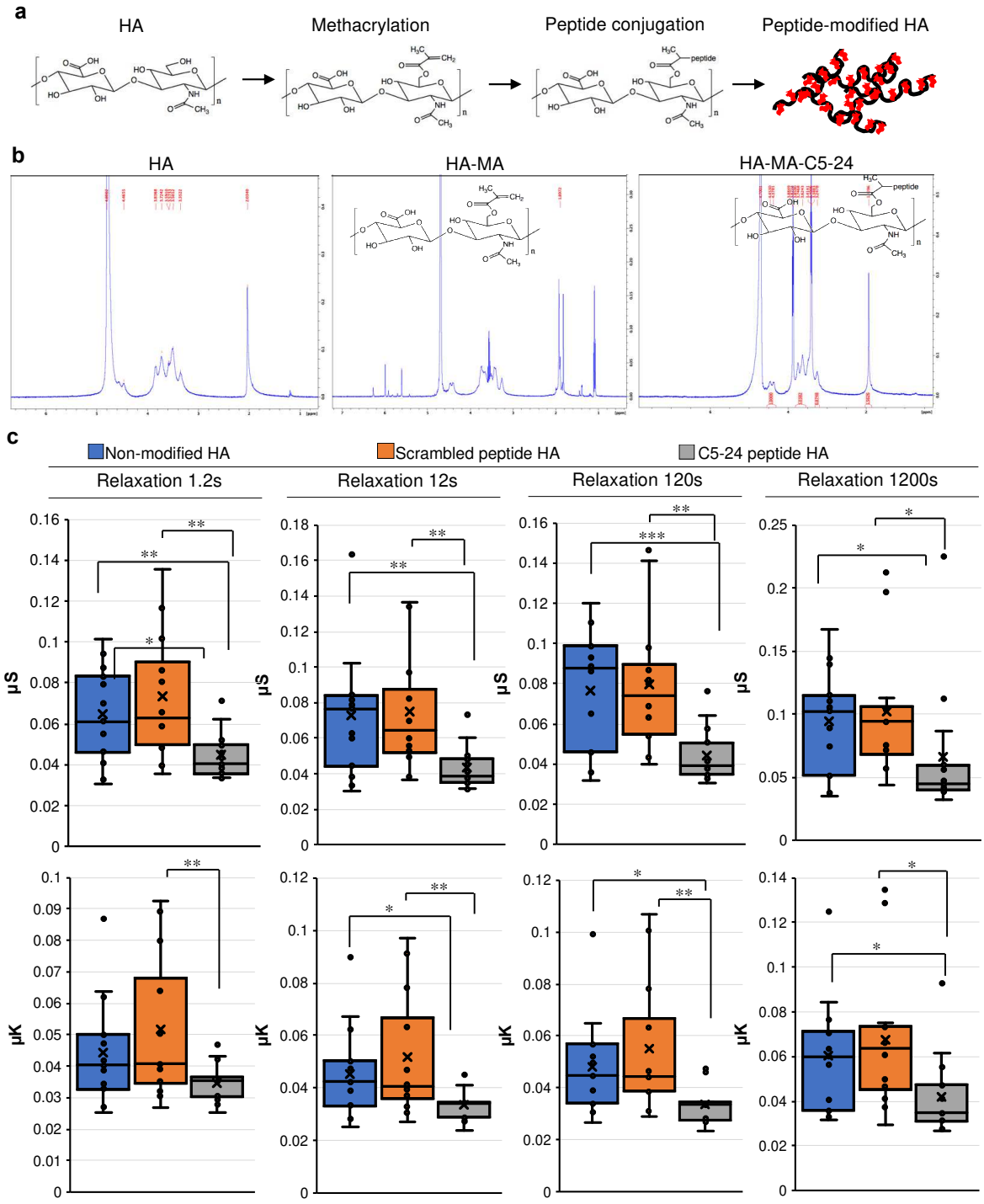

Fig. 3. Application of C5-24 peptides in joint lubrication. (a) For preparation of peptide-conjugated HA. C5-24 peptides or scrambled peptides plus GGGC sequences at the C-terminus were synthesized and conjugated with HA through Michael-addition chemistry. **(b)** In the ^{1}H proton NMR analysis, the methacrylate (MA) and peptide modified HA were dissolved in D_2O and

examined by NMR, with the ^{2}HOH peak at 4.8 ppm used as the reference line. The proton-NMR of the original HA and modified HA revealed distinct methylene (6.0 and 5.6 ppm) and methyl resonances (1.8 ppm) (thin yellow circle indicates the corresponding resonance of the branched group). **(c)** For rheological lubrication measurement of peptide-modified HA, the static (μ_s) and kinetic (μ_k) friction coefficients were examined in paired human OA cartilage cylinder discs collected from OA patients. The cartilage discs were immersed in 1% HA (non-modified) or peptide modified HA solution (including modified C5-24 peptides or scrambled peptides) for 2 h, washed, mounted onto specific plates, and immersed in phosphate-buffered saline (PBS). The cartilage discs were subjected to a pre-conditioning stage for 3600 s and then to four stages of relaxation period, which minimized the cartilage disc height change and reduced the factors influencing the friction measurement in the rheometric program.

are placed in the supplementary information (Fig. S9-Fig. S13), showing the same scenario with the gradual loss of cartilage disc height in the 3600 s relaxation time in the pre-conditioning stage, but returning to consistent cartilage disc height in the following four stages of the relaxation period, which reduced the factors affecting the friction measurement. Together, these data suggest the applicability of C5-24 peptides in the development of novel and effective joint lubricants for OA.

Application in OA regenerative medicine

C5-24-HA may be applied to MSC regenerative medicine by binding to CD44, the HA receptor, which is extensively expressed on the MSC cell surface, and delivering MSCs to the OA cartilage surface. Moreover, the chondrogenic activity of HA is likely to induce MSC chondrogenesis, as demonstrated previously[14,15]. To demonstrate this, rat MSCs were fed with SPIO for subsequent tracking and incubated with fluorescent-conjugated C5-24-HA or scrambled-HA (Fig. 4a). Fluorescence microscopic observation demonstrated that MSCs were tightly surrounded by green fluorescence (Fig. 4b). Furthermore, after incubation with C5-24-HA or scrambled-HA, MSCs were immediately injected into OA joints in a rat model, and the joints were subjected to histological examination 8 weeks post-transplantation. Histomorphometric analysis revealed the successful induction of OA when compared OA group with sham control group (Fig. 4c, 4d).

Moreover, knee joints receiving MSCs delivered by C5-24-HA had apparent cartilage regeneration and safranin-O staining (Fig. 4c), while those receiving MSCs delivered by scrambled-HA still exhibited severe OA, showing multiple cracks on the surface of the cartilage with the loss of safranin-O staining. Quantification of OA degree by modified Mankin score[7] also revealed that the former had better improvement in OA than the latter (Fig. 4d). For cell tracking of SPIO-fed MSCs

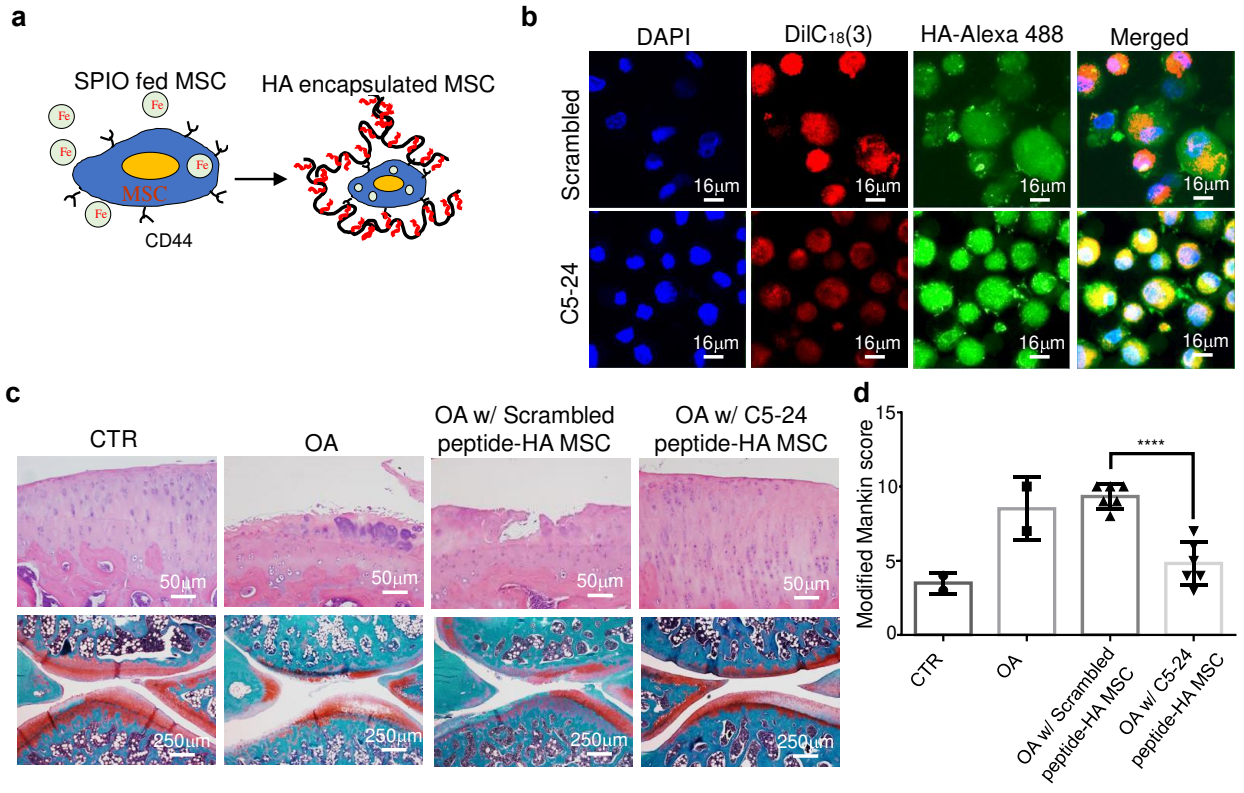

Fig. 4. Application of C5-24 peptides in OA regenerative medicine. Intra-articular injection of SPIO-labeled MSCs delivered in peptide-conjugated HA for the treatment of OA in a rat model. **(a)** For preparation of peptide-modified HA and encapsulation of MSCs, SPIO-fed MSCs were incubated with C5-24-HA or scrambled-HA for 30 min at 37°C, followed by immediate intra-articular injection. **(b)** To obtain confocal images of SPIO-labeled MSCs encapsulated in C5-24-HA, the MSCs were first labeled with $DiIC_{18}(3)$, and incubated with Alexa-488-conjugated HA, followed by microscopic observation with 4′,6-diamidino-2-phenylindole (DAPI) counterstaining. **(c)** Hematoxylin and eosin (H & E) stain (upper panel) and safranin-O/fast green (lower panel) staining of joints collected 8 weeks post-transplantation with MSCs. **(d)** Analysis of OA degrees with modified Mankin's scores according to slides from H & E and safranin-O/fast green staining.

transplanted into the OA joint, rats were subjected to MRI scanning (Fig. S14a) and Prussian blue staining (Fig. S14b), 3 d post-transplantation, revealing specific homing of MSCs to OA cartilage in the C5-24-HA-assisted group, but not in the scrambled-HA-assisted group. These data suggest the applicability of C5-24-HA for enhancing MSC regenerative medicine.

Identification of binding proteins

To identify the putative target protein derived from human OA cartilage tissue that binds to C5-24 peptide, we used biotinylated C5-24 peptide combined with a chemical cross-linker, 3,3'-Dithiobis(sulfosuccinimidylpropionate) (DTSSP), and subsequent sodium dodecyl sulfate-polyacrylamide gel electrophoresis (SDS-PAGE) and liquid chromatography with tandem mass spectrometry (LC-MS/MS) to identify the binding target (Fig. 5a). Silver staining revealed several sharp bands, such as coimmunoprecipitated proteins COIP-1, COIP-3, and COIP-5 (Fig. 5b), which were separately collected, digested with trypsin, and analyzed by LC-MS/MS. The fragments were identified by searching the Swiss Protein Database through algorithms using MASCOT and TurboSequest search engines (Table S3). We found several candidate proteins, including collagen alpha-1 (XII) and collagen alpha-3 (VI) fragments with a probability score, indicating the probability of that peptide belongs to a protein, of up to 850 and 372, respectively, higher than most of the other identified peptides. To further confirm these protein fragments as the target protein of the C5-24 peptide, we examined the mutual binding activities between the target protein and biotinylated C5-24 peptide using ELISA. We first pre-coated the ELISA plate with a specific collagen concentration, to identify the optimal collagen concentration for peptide binding (Fig. 5c), and subsequently used the collagen alpha-1(XII) at 3.3 μg/mL to examine peptide binding (Fig. 5d). We found that biotin-C5-24 peptides bound to collagen alpha-1(XII) and collagen alpha-3 (VI)

fragments, but biotin-scrambled peptides did not. However, a mutual dose-dependent binding was observed only between collagen alpha-1(XII) and biotin-C5-24 peptide (Fig. 5c, 5d). In addition, there was no difference in the binding of biotin-C5-24 peptide and biotin-scrambled peptide to Bovine Serum Albumin (BSA). Together, these data suggest that collagen alpha-1(XII) is the target protein of the C5-24 peptide.

To predict the structure of the protein–peptide complex, the protein–peptide docking was approached through homology modeling (Fig. S15) and the establishment of several reliable structure models targeting human collagen XII (Fig. S16), based on searching for sequence similarities. These structural models were subsequently applied to calculate the possible molecular docking poses with C5-24 and C5-91 peptide chains (Fig. S17 showing the Collagen XII L1385 - S2295 template and Fig. S18 showing the Collagen XII C-terminus S2506 – P2724 domain), which were both the most promising peptide chains and could be selected for further experiments in our study. The protein-peptide docking models were mainly based on an algorithm in compliance with the lowest Gibbs free energy and chemical thermodynamics, after peptide chain binding with the target protein. Our data showed that both C5-24 and C5-91 peptide chains were targeted to the pocket site of collagen XII in the region of L1385 - S2285 with pose 125 and pose 68, and targeted to the C-terminus of S2506 - P2724 with pose 34 and 42, respectively, which share identical docking sites for C5-24 and C5-91 with the highest pose frequencies (Fig. 5e). Furthermore, these predicted poses share the important consensus binding motifs, WXPXW, which may dominate the major docking affinity between peptide chains and collagen XII. In addition, the sequence homology of collagen XII between humans, swine, rabbits, rats, and mice reached 90.3% similarity and 83.7% identity (Fig. S19), and phylogenic analysis revealed a high genetic correlation of *Collagen XII* between these five species. Fig. S20 demonstrates that C5-24 peptides were highly

reliable in rodent, rabbit, and swine OA model examinations. Moreover, according to the consensus domains labeled in colored letters in Table S1, the peptide sequences in the same groups shared important and identical motifs, such as FVEW and DTH in groups 1 and 3, respectively.

Finally, we demonstrated the exclusive expression of collagen XII in OA articular cartilage. The expression of collagen XII was only observed in rat OA cartilage, but not in normal articular cartilage (Fig. S21). In addition, the expression of collagen XII was only observed in human OA cartilage, but not in human non-OA cartilage (Fig S22). Consistent with the area where C5-24 peptide binds (Fig. 1a), collagen XII is mainly expressed in the territorial regions of clustered chondrocytes (Fig. S22). These data are also supported by a cohort study that included 161 OA patients and 29 non-OA patients. The preliminary analysis revealed a significant increase in COL12A1 mRNA levels in combined OA hip and OA knee cartilage relative to the non-OA cartilage[16].

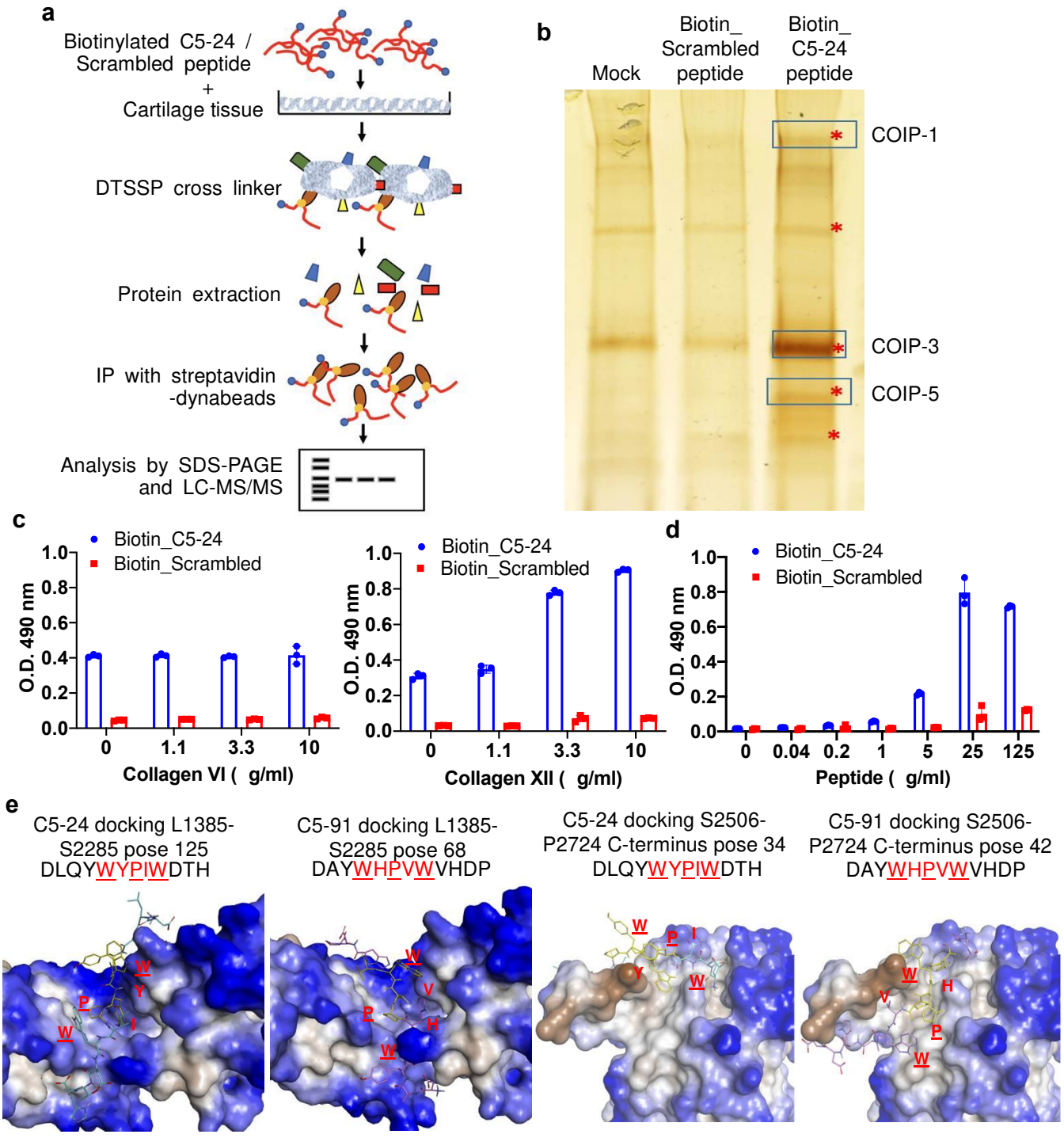

Figure 5. Identification of the binding protein of C5-24 peptides. (a) Schematic diagram of the experimental design to identify the putative target binding-protein in human OA cartilage. **(b)** The C5-24 peptide-targeting proteins in human OA cartilage were isolated by gradient SDS-PAGE, followed by LC-MS/MS analysis. Bands in SDS-PAGE were detected by silver staining. **(c)** For examination of the binding activity of C5-24 peptide with the target-protein by direct ELISA, the ELISA plates were precoated with recombinant human collagen alpha-3 (VI) and alpha-1(XII) proteins at the indicated concentration to determine the optimal collagen concentration for peptide

binding. The peptide concentration used in this experiment was fixed at 25 μg/mL. **(d)** Subsequently, collagen alpha-1(XII) at 3.3 μg/mL was selected to coat the ELISA plate, followed by incubation with C5-24 peptides and scrambled peptides using the indicated concentration. ELISA plates precoated with BSA were served as controls. The biotinylated DYLWQYPDITWH peptides, which is not able to bind to OA cartilage, which was used as a scrambled peptide, and the sequence was identical throughout the study. **(e)** In docking site prediction using homology modeling, human Collagen XII models were established through homology modeling and served as templates for docking pose prediction of candidate peptide sequences. The predicted poses were based on the consensus region in Collagen XII for C5-24 and C5-91 and the highest pose frequencies. The important consensus binding motifs, WXPXW shared between C5-24 and C5-91, were labeled in red and X indicates non-specific amino acid.

Application in disease-modifying OA drugs (DMOADs)

No drugs are currently approved DMOADs. OA therefore can be a serious disease with an unmet medical need for therapies that modify its underlying pathophysiology and translate to long-term, clinically relevant benefits[17]. Currently, there are several drugs in phases II OR III or in the preclinical stage, including fibroblast growth factor-18 (Sprifermin) targeting cartilage regeneration[18]**,** and Kartogenin that promotes the dissociation and nucleus internalization of core binding factor beta (CBFβ) and stimulates cascaded chondrogenesis[19]. All of these developing DMOADs could be further assisted by OA-targeted peptides developed in this study to accelerate delivery to OA tissues. Besides, most of these drugs are focused on an intra-articular route of administration as opposed to systemic pharmacotherapy, aiming to enhance the local bioavailability of drugs and bypass conventional barriers, and to minimize systemic toxicity and enhance safety profile by reducing off-target effects. It is however, important to recognize the marked placebo effect from local intra-articular administration, making the assessment of efficacy more challenging. Improvements in the precision of technology applied to deliver therapeutic agents to OA sites, such as the peptide discovered in this study may lead to the successful development of effective therapies for OA. Future efforts should be directed at delivering disease-modifying drugs in a sophisticated carrier equipped with an OA-targeting peptide to enhance the

development of DMOADs.

We have identified several phage-encoded peptide motifs (WXPXW and DTH) that home selectively to an OA joint without any significant targeting to other articular soft tissues, including synovial tissues, meniscus, and ligaments. Moreover, we identified C5-24 and C5-91 peptides that specifically bind to the territorial region of chondrocytes in OA joints. C5-24 has been successfully conjugated to SPIO and HA for OA diagnosis and lubrication purposes, respectively. Although the C5-91 peptide has not been confirmed to deliver diagnostic agents or lubricants to the articular surface in OA joints, C5-91 peptide was considered to have the same function since it has the same size and shares the same motif as C5-24 peptides.

Although collagen II is the basis for hyaline cartilage, making up 85–90% of all protein in articular cartilage, aging or OA leads to its damage, starting around chondrocytes (territorial region) at the articular surface, and extending into the whole cartilage with progressive degeneration[20]. Given that collagen II is not specifically expressed in OA, collagen II-targeting peptides may not be applied in OA diagnostics, therapeutics, lubrication, and regenerative medicine[21]. In contrast, OA-targeting peptides sharing the binding motif WXPXW were experimentally and *in silico* demonstrated to home selectively to territorial regions and bind to collagen XII that is exclusively expressed in OA cartilage as demonstrated in the current study. Immunofluorescence studies with the antibody demonstrated that collagen XII is localized in collagen I-containing dense connective tissue structures such as tendons, ligaments, perichondrium, and periosteum in embryonic tissues[22], suggesting its emergence during articular joint degeneration and regeneration. Further studies are needed to clarify the role of collagen XII in OA regeneration.

Although peptides that bind to collagen XII were developed for diagnosis, lubricant and regenerative medicine in OA, they may be suitable for other diseases, such as corneal ulcers and perforations that may occur in severe dry eye[23], or injuries or degenerative diseases involving other tissues containing hyaline cartilage, such as intervertebral discs[24] and tracheal cartilage[25]. For example, collagen XII, expressed in Bowman's layer of cornea[26], is overexpressed during corneal ulcer and scar formation[27], therefore the functionalized collagen XII targeting peptides can help the delivery of lubricants, anti-inflammatory drugs and stem cells for the treatment of corneal ulcers. In conclusion, we developed a novel delivery platform targeting collagen XII for improving OA lubrication, diagnosis, treatment, and regenerative medicine. The platform can also be used to treat other diseases, such as eye ulcers and diseases involving other tissues containing hyaline cartilage.

Methods

Provided in the supplementary information.

References

1 Peat, G., McCarney, R. & Croft, P. Knee pain and osteoarthritis in older adults: a review of community burden and current use of primary health care. *Ann Rheum Dis* **60**, 91-97 (2001).

2 Brittberg, M. *et al.* Treatment of deep cartilage defects in the knee with autologous chondrocyte transplantation. *N Engl J Med* **331**, 889-895, doi:10.1056/NEJM199410063311401 (1994).

3 Wakitani, S. *et al.* Safety of autologous bone marrow-derived mesenchymal stem cell transplantation for cartilage repair in 41 patients with 45 joints followed for up to 11 years and 5 months. *J Tissue Eng Regen Med* **5**, 146-150, doi:10.1002/term.299 (2011).

4 Wei, C. C., Lin, A. B. & Hung, S. C. Mesenchymal stem cells in regenerative medicine for musculoskeletal diseases: bench, bedside, and industry. *Cell Transplant* **23**, 505-512, doi:10.3727/096368914X678328 (2014).

5 Yubo, M. *et al.* Clinical efficacy and safety of mesenchymal stem cell transplantation for osteoarthritis treatment: A meta-analysis. *PLoS One* **12**, e0175449, doi:10.1371/journal.pone.0175449 (2017).

6 Jo, C. H. *et al.* Intra-articular Injection of Mesenchymal Stem Cells for the Treatment of Osteoarthritis of the Knee: A 2-Year Follow-up Study. *Am J Sports Med* **45**, 2774-2783, doi:10.1177/0363546517716641 (2017).

7 Chiang, E. R. *et al.* Allogeneic Mesenchymal Stem Cells in Combination with Hyaluronic Acid for the Treatment of Osteoarthritis in Rabbits. *PLoS One* **11**, e0149835, doi:10.1371/journal.pone.0149835 (2016).

8 Murphy, J. M., Fink, D. J., Hunziker, E. B. & Barry, F. P. Stem cell therapy in a caprine model of osteoarthritis. *Arthritis Rheum* **48**, 3464-3474, doi:10.1002/art.11365 (2003).

9 Kamei, G. *et al.* Articular cartilage repair with magnetic mesenchymal stem cells. *Am J Sports Med* **41**, 1255-1264, doi:10.1177/0363546513483270 (2013).

10 Chen, W. H. *et al.* In vitro stage-specific chondrogenesis of mesenchymal stem cells committed to chondrocytes. *Arthritis Rheum* **60**, 450-459, doi:10.1002/art.24265 (2009).

11 Charafe-Jauffret, E. *et al.* Immunophenotypic analysis of inflammatory breast cancers: identification of an 'inflammatory signature'. *J Pathol* **202**, 265-273, doi:10.1002/path.1515 (2004).

12 Deng, M. W. *et al.* Cell Therapy With G-CSF-Mobilized Stem Cells in a Rat Osteoarthritis Model. *Cell Transplant* **24**, 1085-1096, doi:10.3727/096368914X680091 (2015).

13 Singh, A. *et al.* Enhanced lubrication on tissue and biomaterial surfaces through peptide-mediated binding of hyaluronic acid. *Nat Mater* **13**, 988-995, doi:10.1038/nmat4048 (2014).

14 Wu, S. C., Chang, J. K., Wang, C. K., Wang, G. J. & Ho, M. L. Enhancement of chondrogenesis of human adipose derived stem cells in a hyaluronan-enriched microenvironment. *Biomaterials* **31**, 631-640, doi:10.1016/j.biomaterials.2009.09.089 (2010).

15 Chung, C. & Burdick, J. A. Influence of three-dimensional hyaluronic acid microenvironments on mesenchymal stem cell chondrogenesis. *Tissue Eng Part A* **15**, 243-254, doi:10.1089/ten.tea.2008.0067 (2009).

16 Johnson, K., Reynard, L. N. & Loughlin, J. Functional characterisation of the osteoarthritis susceptibility locus at chromosome 6q14.1 marked by the polymorphism rs9350591. *BMC Med Genet* **16**, 81, doi:10.1186/s12881-015-0215-9 (2015).

17 Karsdal, M. A. *et al.* Disease-modifying treatments for osteoarthritis (DMOADs) of the knee and hip: lessons learned from failures and opportunities for the future. *Osteoarthritis Cartilage* **24**, 2013-2021, doi:10.1016/j.joca.2016.07.017 (2016).

18 Shkhyan, R. *et al.* Drug-induced modulation of gp130 signalling prevents articular cartilage degeneration and promotes repair. *Ann Rheum Dis* **77**, 760-769, doi:10.1136/annrheumdis-2017-212037 (2018).

19 Johnson, K. *et al.* A stem cell-based approach to cartilage repair. *Science* **336**, 717-721, doi:10.1126/science.1215157 (2012).

20 Hollander, A. P. *et al.* Damage to type II collagen in aging and osteoarthritis starts at the articular surface, originates around chondrocytes, and extends into the cartilage with progressive degeneration. *J Clin Invest* **96**, 2859-2869, doi:10.1172/JCI118357 (1995).

21 Rothenfluh, D. A., Bermudez, H., O'Neil, C. P. & Hubbell, J. A. Biofunctional polymer nanoparticles for intra-articular targeting and retention in cartilage. *Nat Mater* **7**, 248-254, doi:10.1038/nmat2116 (2008).

22 Sugrue, S. P. *et al.* Immunoidentification of type XII collagen in embryonic tissues. *J Cell Biol* **109**, 939-945, doi:10.1083/jcb.109.2.939 (1989).
23 Deswal, J., Arya, S. K., Raj, A. & Bhatti, A. A Case of Bilateral Corneal Perforation in a Patient with Severe Dry Eye. *J Clin Diagn Res* **11**, ND01-ND02, doi:10.7860/JCDR/2017/24149.9645 (2017).
24 Rustenburg, C. M. E. *et al.* Osteoarthritis and intervertebral disc degeneration: Quite different, quite similar. *JOR Spine* **1**, e1033, doi:10.1002/jsp2.1033 (2018).
25 Roberts, C. R. & Pare, P. D. Composition changes in human tracheal cartilage in growth and aging, including changes in proteoglycan structure. *Am J Physiol* **261**, L92-101, doi:10.1152/ajplung.1991.261.2.L92 (1991).
26 Wessel, H. *et al.* Type XII collagen contributes to diversities in human corneal and limbal extracellular matrices. *Invest Ophthalmol Vis Sci* **38**, 2408-2422 (1997).
27 Massoudi, D. *et al.* NC1 long and NC3 short splice variants of type XII collagen are overexpressed during corneal scarring. *Invest Ophthalmol Vis Sci* **53**, 7246-7256, doi:10.1167/iovs.11-8592 (2012).

Acknowledgements: The authors thank Ms. Ching-Chun Lin and the Core Facility of the Institute of Cellular and Organismic Biology (ICOB), Academia Sinica, for their assistance in C5-24, scrambled peptide synthesis and biotin conjugation. This work was supported by the "Drug Development Center, China Medical University" from The Featured Areas Research Center Program within the framework of the Higher Education Sprout Project by the Ministry of Education (MOE) in Taiwan. We thank to Dr. Wen-Tau Juan and Guan-Yu Zhuo for their assistance in "Two photon core facility, China Medical University".

Grant support: This work was financially supported by Minister of Science and Technology (MOST 106-2321-B-039 -003; 109-2321-B-039 -003). The funding sources had no involvement in study design, in the collection, analysis and interpretation of data, in the writing of the report, and in the decision to submit the article for publication.

Author contributions:

C.-Y. L.: Writing- Original draft preparation, Writing - Review & Editing, Methodology, Experiments conduction, Data analysis; Y.-L. W.: Experiments conduction, Data analysis; Y.-H. C.: Experiments conduction, Data analysis; L. Y. C.: Experiments conduction, Data analysis; G.-W. C.: Computational analysis; H.-C. H.: Funding acquisition, IRB protocol conduction; D. W. H. MRI methodology, Data analysis; H.-C. W.: Conceptualization, Methodology; S.-C. H.: Writing- Original draft preparation, Writing - Review & Editing, Conceptualization, Methodology, Data analysis, Funding acquisition.

Competing interests:

The authors declare no competing financial interests.

SUPPLEMENTARY INFORMATION

Osteoarthritis-targeting peptides aid theranostics and regenerative medicine in osteoarthritis

Chin-Yu Lin[1,#], Yung-Li Wang[1,#], Yi-Hsuan Chi[2], Long Yi Chan[1], Kuan-Wen Chen[3], Horng-Chaung Hsu[4, 5], Dennis W Hwang[7], Han-Chung Wu[2]*, Shih-Chieh Hung[1, 5, 6]*

[1]Institute of New Drug Development, School of Medicine, China Medical University, Taichung, 40402, Taiwan
[2]Institute of Cellular and Organismic Biology, Academia Sinica, Taipei 11529, Taiwan
[3]Molecular Science Center, GGA Corporation, Taipei 11494, Taiwan
[4]Department of Medicine, School of Medicine, China Medical University, Taichung, 40402, Taiwan
[5]Department of Orthopaedics, China Medical University Hospital, Taichung, 40447, Taiwan
[6]Integrative Stem Cell Center, China Medical University Hospital, Taichung, 40447, Taiwan
[7]Institute of Biomedical Sciences, Academia Sinica, Taipei 11529, Taiwan

[#]Equal contribution

*To whom correspondence should be addressed: Shih-Chieh Hung (hung3340@gmail.com) and Han-Chung Wu (hcw0928@gate.sinica.edu.tw)
Shih-Chieh Hung, M.D. Ph.D., Distinguished Professor & Director, Institute of New Drug Development, China Medical University, No.91 Hsueh-Shih Road, North District, Taichung, 40402, Taiwan.
Tel: (+886)4-2205-2121#7728; Fax: (+886)4-2233-3922; E-mail: hung3340@gmail.com

Supplementary Methods

Preparation of cartilage specimens for biopanning and ELISA screening

To avoid interference from individual differences among patients, we used surgical articular cartilage specimens from the same OA patient for the five rounds of biopanning in a phagedisplay experiment. The following processes were used to ensure that the particle-size composition of the cartilage used for the five rounds of biopanning was consistent. A human surgical OA specimen weighed 3.2 g was added to two volumes of phosphate-buffered saline (PBS) and homogenized. The cartilage homogenate was centrifuged at 800 × g and 4°C for 10 min, and the precipitate was collected as "the large particle cartilage sample (C1)". The supernatant was added to a new centrifuge tube, followed by centrifugation at 1,500 × g and 4°C for 10 min, and the pellet was collected as "the cartilage sample with medium particles (C2)". Following centrifugation of the supernatant again at 2,000 × g and 4°C for 10 min, the precipitate was collected as "the small-particle cartilage sample (C3)". The supernatant at this time was separately collected as the "cartilage tissue lysate" for another five rounds of biopanning, which was different from the biopanning performed on the "cartilage tissue pieces". For "cartilage tissue lysate" biopanning, C1, C2, and C3 were weighed and aliquoted into five equal parts, respectively. Each round of biopanning used a mixture of an aliquot of the C1, C2 and C3, for five rounds.

For "cartilage tissue pieces" bio-panning, the cartilage specimens were also cut into square pieces (5 × 5 mm in size) and adhered to a 96-well ELISA plate with nail polish, one piece per well, for the chondrocyte binding screening (Fig. S1a).

Bio-panning of phage clones targeting OA cartilage tissue lysate and pieces

For "cartilage tissue lysate" biopanning, the tissue lysate supernatant was diluted ten-fold with coating buffer [0.1 M $NaHCO_3$, pH 8.6] and coated fresh on 10-cm Petri dishes for biopanning (and 96-well ELISA plates for screening) at 4°C for 24 h before use. The tissue lysate-coated plate was blocked with 1% BSA in PBS at 4°C overnight, 10^{11} pfu of the Ph.D.-12™ phage (New England BioLabs, Ipswich, MA, USA) display peptide library was added and incubated at 4°C for 1 h. After washing, the bound phages were eluted with 1 ml of the log-phase ER2738 culture at 37°C with 100 rpm shaking for 20 min. This eluted phage pool was amplified

and titrated in an ER2738 overnight culture. The recovered phages were used as input for the next round of panning (Fig. S1b), and total 130 phage clones were randomly selected from the fifth round of biopanning to be cultured for ELISA screening.

The processed cartilage specimen was blocked with 1% bovine serum albumin (BSA) in PBS at 4°C for 1 h for each round of "cartilage tissue pieces" biopanning. The Ph.D.-12^{TM} (New England BioLabs, Ipswich, MA, USA) phage display peptide library, which initially contained 10^{11} plaque-forming units (pfu), was added and incubated at 4°C for 1 h. After washing, the bound phages were eluted with 1 ml of log-phase *Escherichia coli* ER2738 culture (New England BioLabs) at 37°C with 100 rpm shaking for 30 min. This eluted phage pool was amplified and titrated in an ER2738 overnight culture. The recovered phages were used as input for the next round of panning (Fig. S1c), and total 95 phage clones were randomly selected from the fifth round of biopanning to be cultured for ELISA screening.

Identification of amino acid sequence motifs to target OA cartilage

The binding activity of the selected phage clones to cartilage tissue lysate (Fig. S2c) and cartilage tissue pieces (Fig. S2d) was examined by ELISA. Phage clones with the highest binding affinity (A490 value > 0.15 for the cartilage tissue lysate and A490 value > 2.0 for the cartilage tissue piece) were selected and sequenced. We identified five distinct groups with differing consensus motifs by amino acid sequence alignment (highlighted in Table 1).

Validation of peptides targeting OA cartilage using immunofluorescence of hPi-GL chondrocyte cell line

For examination of those phage clones, slide-cultured hPi-GL cells were fixed with 4% paraformaldehyde in PBS at room temperature for 15 min, washed with PBS and permeabilized with 0.1% Triton X-100 at room temperature for 30 min, blocked for nonspecific binding with 1% BSA/PBST. The slide-cultured hPi-GL cells were separately incubated with 4×10^8 pfu, 8×10^8 pfu, and 10^9 pfu selected phage clones at 4°C for 1 h. After removing the unbound phages by washing, the cells were incubated with anti-M13 mouse mAb (GE Healthcare, Milwaukee, WI, USA) as the primary antibody and R-Phycoerythrin-AffiniPure F(ab')2 fragment goat anti-mouse IgG (Jackson ImmunoResearch Inc.) as the secondary antibody at room temperature for 1 h, respectively. Then, washed with PBST, and counterstained with Hoechst 33258 (1 μg/ml; Sigma-Aldrich) at

room temperature for 10 min. The cells were analyzed for phage binding and localization by fluorescence using confocal microscopy (Zeiss LSM 700).

Selection of peptides targeting OA cartilage but not synovium and meniscus

To examine localization of the targeting phages bound to articular tissues, human OA cartilage specimens were used for examination. Paraffin-embedded human OA tissue, synovium, and meniscus sections were retrieved from specimens of human OA surgical treatment under the approval of the Institutional Review Board of China Medical University Hospital (IRB no. CMUH108-REC1-046 and T-CMU-23728). Written informed consent was obtained, and all human tissue samples were coded for anonymity. All sections were dried, deparaffinized and rehydrated by standard protocols, and subsequently incubated with C5-87, C5-66, C5-83, C5-91, C5-24, E5-8, and C5-46 phage clones, or the control phage (5×10^8 pfu/μl). After washing, the sections were treated with anti-M13 mouse mAb (GE Healthcare) for 1 h at room temperature. Following several washing steps, a biotin-free super sensitive polymer-HRP detection system (Biogenex, Fremont, CA, USA) was used to detect immunoreactivity. The slides were lightly counterstained with hematoxylin, mounted with Aquatex (Merck, Darmstadt, Germany), and examined by light microscopy. Peptide sequences displayed on the phage clones that exhibited prominent binding to chondrocytes, but not synovium or the meniscus, were selected and synthesized for subsequent studies.

Rat OA model establishment

The OA in rat model was established as previous described with slightly modification (*1*). In brief, the male SD rats ≅ 300 grams in weight were used in this study. All animal experiments were approved by the China Medical University Committee for the Use and Care of Animals. Rats were kept under standard laboratory conditions (temperature 24°, 12h light-dark cycle), fed standard diet and drank tap water. Rats were anesthetized with 2.5% isofluorane (Abott, USA) in 70 ml/min flow rate before every injection. Rat joint OA was induced in the right knees in each group by injecting 0.2 ml of 4% papain solution (Sigma-Aldrich, USA) with 0.1 ml of 0.03 M cysteine (Sigma-Aldrich, USA) as activator. Same amount of saline was injected into the left knees in each group. Injection was repeated on the fourth and seventh days, respectively, and two weeks after the last papain injection, rat knees were removed for histological analysis to confirm the formation

of OA. The established OA model in rats was further used in the following experiments for intraarticular injection.

Preparation of rhodamine labeled C5-24 peptide and 2-phonton microscopic observation

To demonstrate the OA specific targeting activity of C5-24 peptide, the DYLWQYPDITWH peptides, which is not able to bind to OA cartilage, was used as scrambled peptides. The rhodamine-labeled C5-24 and scrambled peptides were separately injected into rat joints without (control) or with enzyme-induced OA (*2*). The C5-24 and scrambled peptides were chemically synthesized as accordingly (ABI, USA), modified with Biotin-PEG_2-Iodoacetyl bridge linker (Thermo Fisher Scientific, USA) in HEPES buffer pH 8.0 through click reaction, further linked with avidin labeled rhodamine (JacksonImmuno, USA) and subjected to dialysis in ddH_2O in M.W. 4K cut-off to remove the unlabeled rhodamine, further lyophilized and stored in -20 °C. Aliquots of 1 μg rhodamine-labeled peptides in 40 μl PBS were used for intraarticular injection with using 30G syringes.

Rat Knees were removed at 1-day post-injection, and both femoral condyles and tibias were cleaned thoroughly, immersed in PBS and sophisticatedly attached on 3.5 cm dish for 2-phonton microscopic observation. The microscope system was operated using a near-infrared femtosecond laser (Mira 900, Coherent, USA) at the central wavelength of 810 nm, 76 MHz pulse repetition rate, and 200 fs pulse width for imaging. The laser power was controlled to 20 mW that is sufficient to produce SHG and TPEF, and also prevented photodamage during continuous illumination. Thus, the wavelength of SHG from collagen fibers is 405 nm, while the TPEF from collagen, elastin, FAD, and NADH is approximately ranging from 450 to 650 nm (*3, 4*). All images were obtained by a laser scanning unit (Fluoview 300, Olympus, Japan), a pair of two objective lenses for both lasers focusing and collection of photons (UPlanSApo 20×/0.75, Olympus, Japan), and two photomultiplier tubes respectively for SHG and TPEF detection (R3896, Hamamatsu, Japan). SHG and TPEF were filtered from the intense excitation laser background by a combination of band-pass filter (FF01-405/10, Semrock, USA) and color glass (BG39, Schott, Germany). And, then splitted by a dichroic mirror (FF435-Di01, Semrock, USA) and forward detected. Note that we used a cube polarizing beam-splitter (GT10-B, Thorlabs, USA) combined with a half (AHWP05M-980, Thorlabs, USA) and a

quarter (AQWP05M-980, Thorlabs, USA) waveplates to demonstrate LP and CP imaging, respectively. Only the extinction ratio of linear polarization larger than 50:1 and the ellipticity of circular polarization (I_{max}/I_{min}) less than 1.1 after the focusing objective lens can then be used for the following two-photon imaging. The acquired images were mainly processed and analyzed with ImageJ/FiJi software (National Institutes of Health, Bethesda, MD, USA). The type II collagen structure reconstructed through the second harmonic generation images (*5*) (Fig. 1a) showed porous collagen fiber inter-connected structures (green color) surrounding nested chondrocytes (black area).

Preparation of C5-24 peptide-conjugated superparamagnetic iron oxide (SPIO) and IR spectroscopy

The C5-24 and scrambled peptides were chemically synthesized, meanwhile aminosilane modified SPIO particles in 50 nm in diameter (Chemicell GmBH, Germany) were firstly crosslinked with succinimidyl-[(*N*-maleimidopropionamido)-tetraethyleneglycol] ester (Thermo Fisher Scientific, USA) in sodium bicarbonate buffer pH 8.5 to form amide bonds, and subsequently interacted with sulfhydryl group on cysteine of the peptides in pH 7.2 to form a stable thioether bond and subjected to dialysis in ddH_2O in M.W. 10K cut-off to remove the free-forms of peptides, bridge linkers and salts, leaving groups and further concentrated in reduced pressure, resuspended in PBS and stored in 4 °C for experiments not longer than 2 weeks. To analyze the installation of peptides on SPIO, a part of prepared SPIOs were lyophilized, grounded with potassium bromide (KBr) thoroughly in 1:100 wt./wt. and compressed in 200 pound/inch^2 to form a thin pellet for further infrared radiation spectroscopic analysis (Perkin Elmer, USA). IR was scanned from 400-4000 1/cm frequency to record the characteristic-group and finger-print region molecular groups in transmission mode, respectively.

Magnetic resonance imaging (MRI) analysis of OA in rat model

Rats at the indicated time points as results shown were anesthetized by inhalation and subjected to MRI scanning. MRI scans were performed using a 4.7T MR scanning system (Bruker BioSpin, Germany) at the Institute of Biomedical Sciences, Academia Sinica in Taiwan. T1-weighted and T2-weighted sagittal sections were rendered using the following settings: fast spin echo sequence with a time to repetition of 2000 ms and time to echo of 72ms; slice thickness was 1 mm; interslice gap 1 mm; matrix 256; TE 60; TR 2000; field of view 60 mm; number of averages 2. A 60 mm volume resonator and a 2 cm diameter surface receive coil were

used to maximize image resolution and quality. Tomographs DICOMs of MRI were analyzed by Osirix MD (Osirix Ltd., USA).

OA in mini-pig model, intraarticular injection of C5-24 peptide-conjugated SPIO and 3T-MRI analysis

For surgery of anterior crucial ligament (ACL) transection to establish OA, a Taiwan Lan-Yu minipig (9-month-old, weight ≈ 50-60 kg) was anesthetized by combined intramuscular (i.m.) injection of Stresnil (20 mg/kg) and atropine sulfate (0.02 mg/kg), followed by i.m. injection of Zoletil® 50 (4 mg/kg, Virbac Animal Health, France) 15 min later. In order to get a more homogenous group of knee joints, only female pigs were included in the current study. During the surgery, the animals continued to be anesthetized with gas containing oxygen (flow rate of 1.5 L/min), nitrous oxide (flow rate of 1 L/min) and 1% isoflurane. The right rear limb was washed and covered sterilely. Following intravenous administration of cefazolin (2 g), an incision in the skin of approximately seven cm was made in the right knee from the patella to the tuberositas tibiae. The joint was then opened medial to the patellar ligament and the patella is partly luxated. The ACL was then fixed by a clamp and cut at the distal end using a scalpel. To avoid spontaneous healing of the ACL after this transection, a proximal resection was additionally carried out using an electrical arthrosector. Following successful rinsing with sterile 0.9% saline solution, the skin incision was closed in layers using 1-0 VICRYL® sutures (Ethicon, USA). The minipigs were able to walk and move normally after this procedure. MRI scans were performed at the indicated time points using a 3T MR scanning system (Achieva x 3.0, Philips, Germany) at the Instrument Technology Research Center, NARLabs in Taiwan. T1-weighted and T2-weighted sagittal sections were rendered using the following settings: time to repetition of 2000 ms and time to echo of 72ms; slice thickness was 3 mm; matrix 512; TE 200; TR 3500; field of view 60 mm; number of averages 2. Tomographs DICOMs of MRI were analyzed by Osirix MD (Osirix Ltd., USA).

Preparation of C5-24 and scramble peptide-conjugated hyaluronic acid (HA)

The peptide conjugated HA was synthesized as previous described with slight modification (*6*). In brief, MeHA was firstly synthesized through the reaction of methacrylic anhydride (94%, M.W. 154.17; Sigma) with 1% (wt/vol) HA (sodium hyaluronate powder, molecular weight ≈ 110-150 kDa; Kikkoman, Japan) in deionized water at pH 8, purification via dialysis (molecular weight cutoff 6–8 kDa), followed by

lyophilization. Methacrylation efficiency of the intermediate MeHA macromer was estimated by ^{1}H NMR. C5-24 and scrambled peptides with a cysteine residue at the C-terminal end to permit the sulfhydryl group to reacted with MeHA through Michael-Addition reaction. MeHA macromers and peptides were dissolved in triethanolamine-buffered saline (TEOA buffer, 0.2 M TEOA, 0.3 M total osmolarity, pH 8.0) and maintained at 37 °C overnight for peptide coupling. The peptide conjugated HA was subjected to dialysis in ddH_2O in M.W. 12K cut-off to remove the free-forms of peptides, TEOA, salts and MA, and further lyophilized and stored in room temperature. The peptides conjugated HA was lysed in 0.1M acid and subjected to ^{1}H NMR to estimate the conjugation efficiency of peptide.

Lubricant performance analysis

Human articular cartilage samples collected from femoral condyles of cartilage were prepared for lubrication testing with a slight modification from previous publishes (*7*). Human osteoarthritic cartilage samples were sectioned from the patients who underwent total knee arthroplasty under stringent supervision by IRB committees from China Medical University Hospital (IRB number: CMUH108-REC1-046, and T-CMU-23728). Care was taken to avoid damaging the articular surface during dissection. The superficial layer of OA cartilage from individual patient was maintained intact, punch-cut to obtain a cylinder disc with diameter in 8.0 mm and 6.0 mm, respectively and only the deep layer of cartilage was cut to obtain a flat disc to glue to the metal counter-surface of the particularly designed testing modules while performing friction measurements in rheometer. Cartilage was used fresh without freezing or the addition of protease inhibitors so as not to change the surface lubrication properties. Samples were washed vigorously in PBS overnight to deplete the cartilage surface of any residual synovial fluid, after which they were separated into at least 3 groups. Cartilage discs were pre-incubated in 1 ml original HA or peptide modified HA (1% HA in PBS) for 2 h as indicated in Results for binding of the nonmodified HA or peptide modified HA with cartilage disc, followed by immersing them in 10 ml PBS in testing modules and mounting onto rheometer (HR-1, TA Instrument Ltd., USA) for friction measurements.

The rheometer was initially set to zero using standard protocol in compliance with manufacturer's instruction, and then we calculated the initial heights of the cartilage samples with an electronic caliper

followed by loading the samples on the rheometer. The samples were glued with cyanoacrylate glue to the top and bottom rheometer fixtures in parallel plate configuration. Only a thin layer of glue bound to the cartilage and metal fixture surface. The 6.0 mm sample surface was positioned on top of the 8.0 mm surface. The top sample was lowered and pressed against the bottom sample until a load value of ~0.01 N to avoid insufficient contacts between the sample surfaces, load value fluctuations and minimize the errors in height measurements. The corresponding recorded height, which was automatically sensed by rheometer, was taken for strain calculation. The instrument was programmed to record the total cartilage thickness and calculate the height for ≈14% compression. The total thickness of the human OA cartilage sample was in the range of ≈2.5 – 3.5 mm, which were tested in a bath of HA/PBS fluid (10 mL) covered with protecting lid to prevent desiccation. Each sample was checked for proper alignment and surface irregularity, and the experiment was performed on samples with flat surfaces. The samples were bathed in the test lubricant, compressed to 86% of their original combined height and preconditioned by rotating two revolutions in each direction at an effective sliding velocity of 0.3 mm/s, which is defined as the angular velocity times the effective radius of the annulus $R_{eff} = 2/3[(R_o^3-R_i^3)/(R_o^2-R_i^2)]$. This preconditioning was repeated twice more, followed by a 3600 seconds stress-relaxation period to allow the pressurization of the fluid in the compressed cartilage to fully subside. The equilibrium normal stress data recording and measurement was performed for each experimental group (Fig S8 ~ Fig. S20). Lubrication testing was performed in 14 stages. The first two stages were considered negligible and used as a clearing or pre-shear stage. Stages 3, 6, 9 and 12 were performed to analyze the effect of different durations of relaxation. Samples were allowed to relax between tests for 1200, 120, 12 and 1.2 seconds. Lubrication data were recorded during stages 4-5, 7-8, 10-11 and 13-14; each stage was in a different direction of rotation and at a constant shear rate. During each test, torque (τ) and axial force (N) were measured, and instantaneous measurements of μk, the kinetic friction coefficient, were determined from the following equation: $\mu k = \tau/(R_{eff} \times N)$. Instantaneous μk values were averaged over the second revolution in each direction to produce an average μk that was used for comparison. Static friction coefficients were calculated as the instantaneous $\mu s = \tau_{max}/(R_{eff} \times N)$ at the maximal torque value found during the startup period of the test. After experimentation a central indentation due to ≈14% compression on the cartilage surface was confirmed.

Rat MSCs isolation and labeling with SPIO, and delivery via C5-24 peptide conjugated HA

Rat MSCs were isolated and expanded as previously described. Briefly, femora collected from 2 female Sprague-Dawley rats with 8 to 10 weeks of age (BioLASCO Taiwan Co Ltd, Taipei, Taiwan), and the soft tissues were detached aseptically. The bone marrow mononuclear cells were isolated by the density gradient centrifugation method and suspended in complete culture medium (CCM: α-MEM supplemented with 16.6% fetal bovine serum, 100 U/mL penicillin, 100 μg/mL streptomycin, and 2 mM L-glutamine), then seeded in culture dishes in the density of $1 \times 10^5/cm^2$. Nonadherent cells were removed by washing and changing medium at 24 hours later. When cells reached sub-confluence, the cells (passage 0) were harvested for further subcultures. Then, the cells were seeded at density of 100 cells/cm^2 and grown in CCM with medium change twice per week. The MSCs used in this study were passage 3-4.

For MSCs labelling with superparamagnetic iron oxide nanoparticles (SPIO), 50 μg/mL of SPIO (Chemicell GmbH, Gemany) was pre-mixed with 0.75 μg/mL poly-L-lysine (Sigma Aldrich, USA) in culture medium at room temperature for 1 h. For endocytosis of SPIO nanoparticles, MSCs were seeded in 6-well plate at density of 4×10^4 / well and grown for 24 h, followed by thoroughly washed with PBS. Then, the MSCs were collected to a microtube and incubated with 2% C5-24 peptide conjugated HA in serum-free medium in concentration of 1×10^6 cells/200 μl at 37˚C for 30 min. For intra-articular injection, the volume of HA encapsulated MSCs was reduced to 25 μl containing 1×10^6 cells, and were sophisticatedly injected into a OA rat knee joint synovium capsule.

Histological, immunocytofluorescent and immunohistochemical analysis and confocal microscopic observation

Histological analysis of HA encapsulated MSCs transplantation, rats were sacrificed at post-transplantation time point as indicated in the results, whole knee joints were removed, fixed with 4% paraformaldehyde (PFA) in PBS, decalcified in 0.5 M EDTA for 2 weeks, embedded in paraffin and serial sectioned in 5 μm thickness in sagittal direction. Serial sections in the mid-zone of femoral condyle were prepared for H&E staining, Prussian blue staining and Safranin-O staining by standard protocol and observed by phase contrast

microscope (Carl Zeiss). For H&E staining, de-paraffined slides were serially rehydrated, stained with Lillie Mayer haematoxylin (Sigma Aldrich, USA) for 10 minutes, followed with eosin Y (Sigma Aldrich, USA) for 30 seconds, finally with serial dehydrated, cleared and mounted. For Prussian blue staining, slides preparation similar to H&E, rehydrated slides were stained with 5% potassium ferrocyanide in 10% HCl solution (Sigma Aldrich, USA) for 20 minutes, countered stained with Fast Red and finalized with dehydrated, cleared and mounted with resinous gel and coverslip. For Safranin-O staining, rehydrated slides were stained with 0.05% Fast Green solution for 3 minutes, followed with 0.1% Safranin-O solution for 5 minutes, and finalized with cleared and mounted with resinous gel.

For confocal microscopic observation of HA encapsulated MSCs, the HA was methacrylated and conjugated with Alexa-488 fluorescent dye, prepared in 2% in PBS. MSCs were collected to a microtube, labeled with Dil3 fluorescent dye (Invitrogen, USA) according to the manufacturer's instruction and incubated with HA solution at 37˚C for 30 min. Subsequently, dropped onto a slide and immediately observed by confocal microscope (Leica), 3D images were reconstructed by ImageJ Fiji (NIH).

Identifying the target protein of the C5-24 peptide by affinity trapping, liquid chromatography-tandem mass spectrometry (LC-MS/MS) and ELISA

To identify the binding target of C5-24 peptide chain, human OA cartilage specimens were homogenized for affinity trapping. The biotinylated C5-24 peptide in 1mg/ml in PBS was added to the cartilage homogenate and incubated at 4°C for 1 h. After washing, the DTSSP solution was added to a final concentration of 2 mM for peptide-target protein cross-linking. The reaction mixture was incubated and rotated at room temperature for 30 min. The reaction was stopped with 1 M Tris base. After lysing the chondrocytes with the first lysis buffer (1 M NaCl in 100 mM Tris acetate, pH 8.0) at 4°C for 24 h, the lysates were centrifuged, and the pellet was re-treated with the second lysis buffer (4 M guanidine HCl, 65 mM DTT, 10 mM EDTA in 50 mM sodium acetate, pH 5.8) at 4°C for another 24 h. Following centrifugation, the guanidine extracts were mixed with 100% ethanol (5:1 volume ratio) at -20°C for 16 h to ensure removal of the residual guanidine HCl. The target protein fraction was precipitated by centrifugation at 16,000 × g and 4°C for 45 min, the pellet was washed with 90% ethanol, dried, and re-dissolved with 100 mM acetic acid containing 100 μg/ml pepsin. MyOne

Streptavidin C1 Dynabeads (Invitrogen, Carlsbad, CA, USA) were added to the protein lysates and mixed thoroughly for 1 h. Immuno-magnetic separation was used to pull down the peptide-protein complexes. Finally, the purified proteins were separated by gradient sodium dodecyl sulfate-polyacrylamide gel electrophoresis (SDS-PAGE) (Bio-Rad) and silver-stained with a SilverQuest Silver Staining Kit (Invitrogen).

The stained protein bands were cut into small pieces and washed with 10mM ammonium bicarbonate (ABC, Sigma, St Louis, MO) containing 50% ACN for 5 min three times. The gel pieces were dehydrated with 100% CAN and rehydrated with 25mM ABC (pH 8.2) solution containing 1 ng/μl trypsin (Promega, Madison, WI) and then incubated at 37 °C overnight. After digestion, the tryptic peptides were extracted from the gel using 1% FA in 50% ACN and dry using a centrifugal concentrator. The peptide fragments were identified by LC-MS/MS. LC-MS/MS was performed using an ion trap mass spectrometer (HCTultra PTM discovery, Bruker, Billerica, MA) coupled online with Ultimate 3000 nanoLC system (Dionex, Sunnyvale, CA). The sample was injected into a trap column (C18, 5 μm, 1mm × 5 mm, Dionex, Sunnyvale, CA) and separated online with a reverse phase column (Atlantis C18, 3 μm, 75 μm × 150 mm, Waters, Milford, MA) at flow rate of 300 nl/ min. Peptides were eluted with H_2O/ACN gradient from 2 to 40% of solvent B (100% ACN, 0.1% FA) in 6 min and 40 to 70% of B in 24 min. MS and MS/MS scan range is 400–1600 m/z and 100–2500 m/z, respectively. Protein candidates were identified by searching the Swiss Protein Database using the MASCOT (Matrix Science, London, UK) and TurboSequest search engines (Thermo Fisher Scientific, Waltham, MA, USA), following validated by ELISA.

Firstly, ELISA plate was coated with collagen alpha-3 (VI) and collagen alpha-1(XII) in coating buffer (0.5M $NaHCO_3$) at room temperature for 2 h and blocked with 5% milk/TBST at 4 °C overnight. The biotinylated peptide was added into ELISA plate and incubated at room temperature for 1 h. The plate was washed with PBS and the biotinylated peptide was probed with HRP-conjugated mouse anti-M13 antibody (GE Healthcare Biosciences). Binding of the biotinylated peptide to the recognized collagen alpha-3 (VI) or collagen alpha-1(XII) was detected by HRP-conjugated streptavidin (Thermo Pierce Biotechnology Scientific). The plate was washed with PBS and subsequently incubated with peroxidase substrate ophenylenediamine dihydrochloride (OPD; Sigma). The reaction was terminated by 3 N HCl, and the absorbance at 490 nm was measured with an ELISA reader.

Homology modeling of C5-24 peptide docking target

Molecular modeling to further confirm the binding target of selected phage clones on cartilage tissue was performed by Dassault Systems (BIOVIA, Discovery Studio Modeling Environment, Release 2019, San Diego, USA) in compliance with the developer's instruction. Briefly, the standard sequence code of human, mouse, and pig ColXII which retrieved from Uniprot Database were Q99715, Q60847, F1RQI0, individually. Three different parts of human ColXII homology models were built using MODELER based on the templates (PDB code: 1FNF, 2B2X, 2UUR) from BLAST result. The length of first human ColXII model was from L1385 to S2285, with 30% identity to the template 1FNF, which indicated the fibronectin structure and could be used to model establishment due to the highly conserved structural topology. The second and third human ColXII models were from K2321 to L2513 and S2506 to P2724 with 31% and 36% sequence identity with template 2B2X and 2UUR, individually. All of the homology models were firstly checked by PDF total energy, DOPE (Discrete Optimized Protein Energy) and verify score, Ramachandran plot and refined the structure to obtain the reasonable backbone and sidechain conformation. The most representative protein templates were used to predict the binding sites and poses with C5-24 and C5-91 peptide chains due to the most promising results in IHC. Subsequently, Protein-peptide docking using ZDOCK was performed for searching the potential binding region. The Z_Dock score and E_R_Dock score were used to validate the docking capability and exactitude between peptides and target protein templates.

Statistical analysis

Data are presented as mean ± SD, statistical comparisons were performed by Student's *t*-test or one-way analysis of variance (ANOVA) and p values <0.05 were considered significant. All calculations were performed using Statistics Analysis System (SAS) licensed to China Medical University. All *in vivo* data are representative of at least 3 independent experiments as indicated.

References

1. N. Murat, B. Karadam, S. Ozkal, V. Karatosun, S. Gidener, [Quantification of papain-induced rat osteoarthritis in relation to time with the Mankin score]. *Acta Orthop Traumatol Turc* **41**, 233-237 (2007).
2. M. W. Deng *et al.*, Cell Therapy With G-CSF-Mobilized Stem Cells in a Rat Osteoarthritis Model. *Cell Transplant* **24**, 1085-1096 (2015).
3. N. R. Liu, G. N. Chen, S. S. Wu, R. Chen, Distinguishing human normal or cancerous esophagus tissue ex vivo using multiphoton microscopy. *Journal of Optics* **16**, 025301 (2014).
4. J. Xu *et al.*, Multiphoton microscopy for label-free identification of intramural metastasis in human esophageal squamous cell carcinoma. *Biomedical Optics Express* **8**, 3360-3368 (2017).
5. M. A. Houle *et al.*, Analysis of forward and backward Second Harmonic Generation images to probe the nanoscale structure of collagen within bone and cartilage. *J Biophotonics* **8**, 993-1001 (2015).
6. L. Bian, M. Guvendiren, R. L. Mauck, J. A. Burdick, Hydrogels that mimic developmentally relevant matrix and N-cadherin interactions enhance MSC chondrogenesis. *Proceedings of the National Academy of Sciences of the United States of America* **110**, 10117-10122 (2013).
7. A. Singh *et al.*, Enhanced lubrication on tissue and biomaterial surfaces through peptide-mediated binding of hyaluronic acid. *Nat Mater* **13**, 988-995 (2014).
8. E. Charafe-Jauffret *et al.*, Immunophenotypic analysis of inflammatory breast cancers: identification of an 'inflammatory signature'. *J Pathol* **202**, 265-273 (2004).

Supplementary Figures

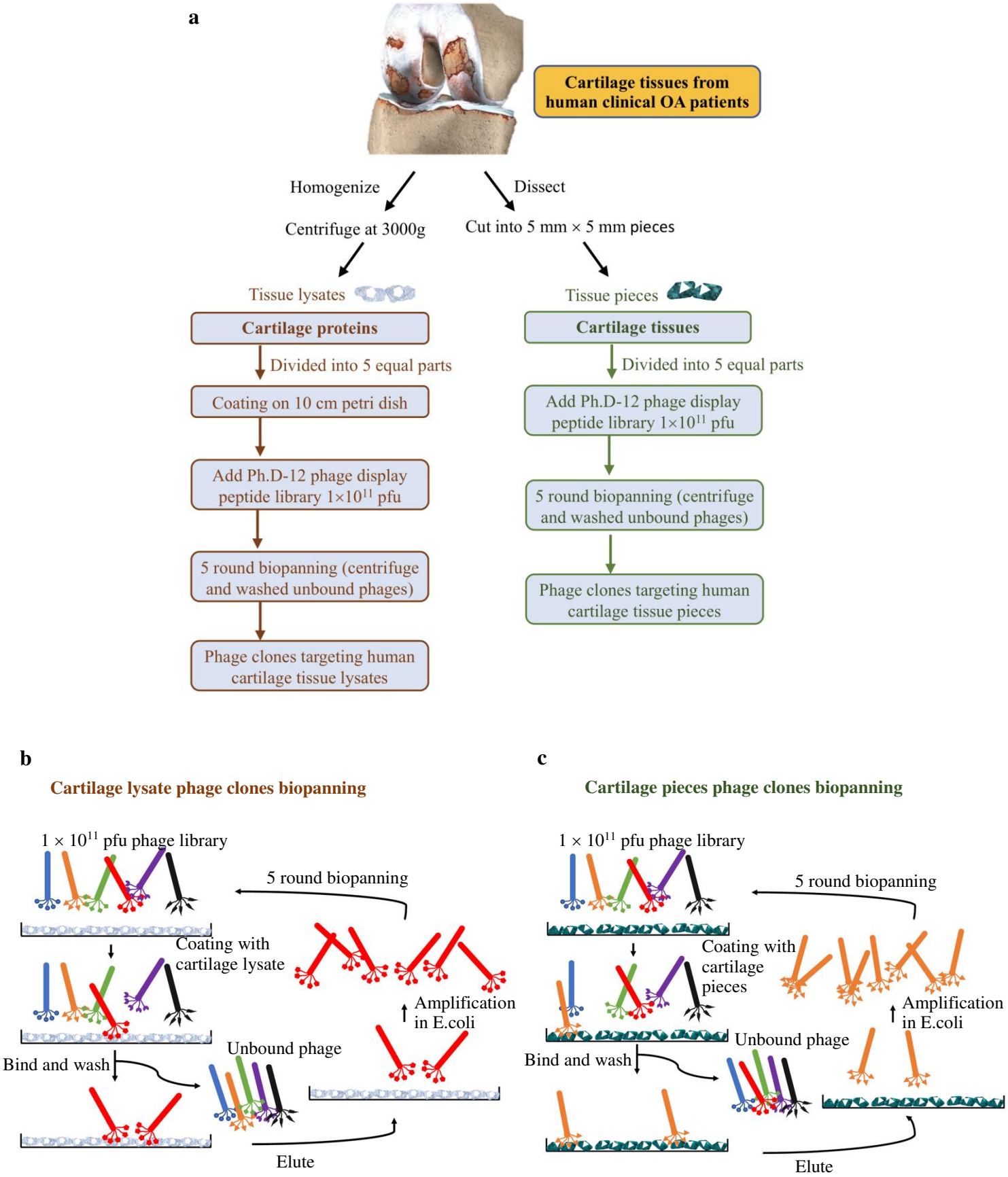

Fig. S1. Biopanning of phage clones targeting OA cartilage. The OA articular cartilage specimens of knee joints from patients who received total knee joint replacement were separated into two parts, cell lysates and

square pieces, for screening a phage peptide display library to identify clones targeting OA cartilage. **(a)** Preparation of clinical cartilage tissues for phage clones biopanning. **(b)** Biopanning of cartilage lysate. **(c)** Biopanning of cartilage pieces.

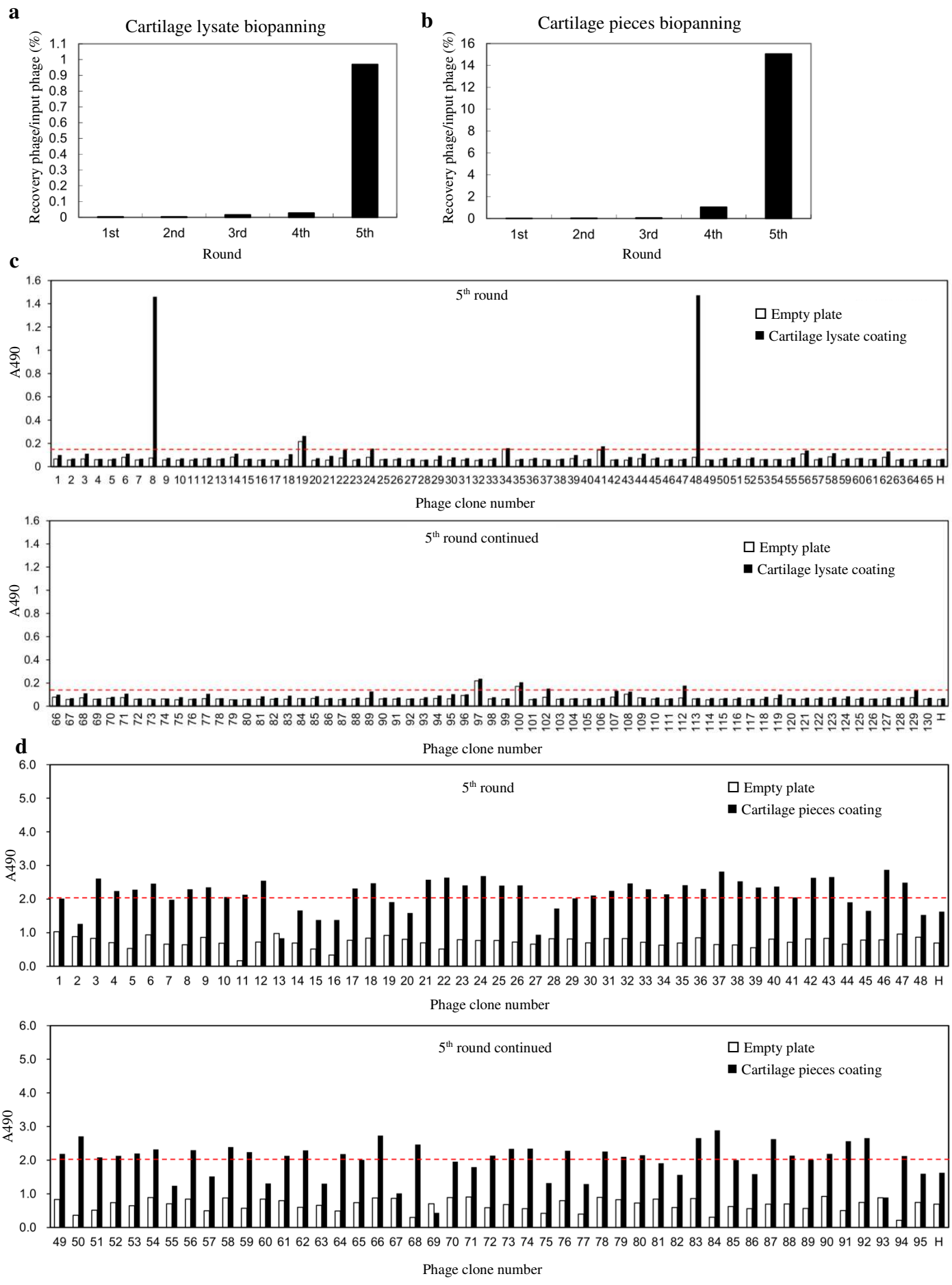
a
Cartilage lysate biopanning
Recovery phage/input phage (%)
1st
2nd
3rd
4th
5th
Round
b
Cartilage pieces biopanning
Recovery phage/input phage (%)
1st
2nd
3rd
4th
5th
Round
c
5th round
Empty plate
Cartilage lysate coating
A490
Phage clone number
5th round continued
Empty plate
Cartilage lysate coating
A490
Phage clone number
d
5th round
Empty plate
Cartilage pieces coating
A490
Phage clone number
5th round continued
Empty plate
Cartilage pieces coating
A490
Phage clone number

Fig. S2. Biopanning to identify the OA-targeting clones through screening of phage-displayed peptide library. **(a)** Recovery of the phage titer improved significantly after five rounds of biopanning for OA cartilage tissue lysate. **(b)** The recovery phage titer increased significantly after five rounds of biopanning for the cartilage tissue pieces. **(c)** ELISA screening of 130 phage clones selected from the fifth round of biopanning (panel A) for human cartilage tissue lysate binding. **(d)** ELISA screening of 95 phage clones selected from the fifth round of biopanning (panel B) for human cartilage tissue pieces binding. Helper phage (H) was used as a negative control.

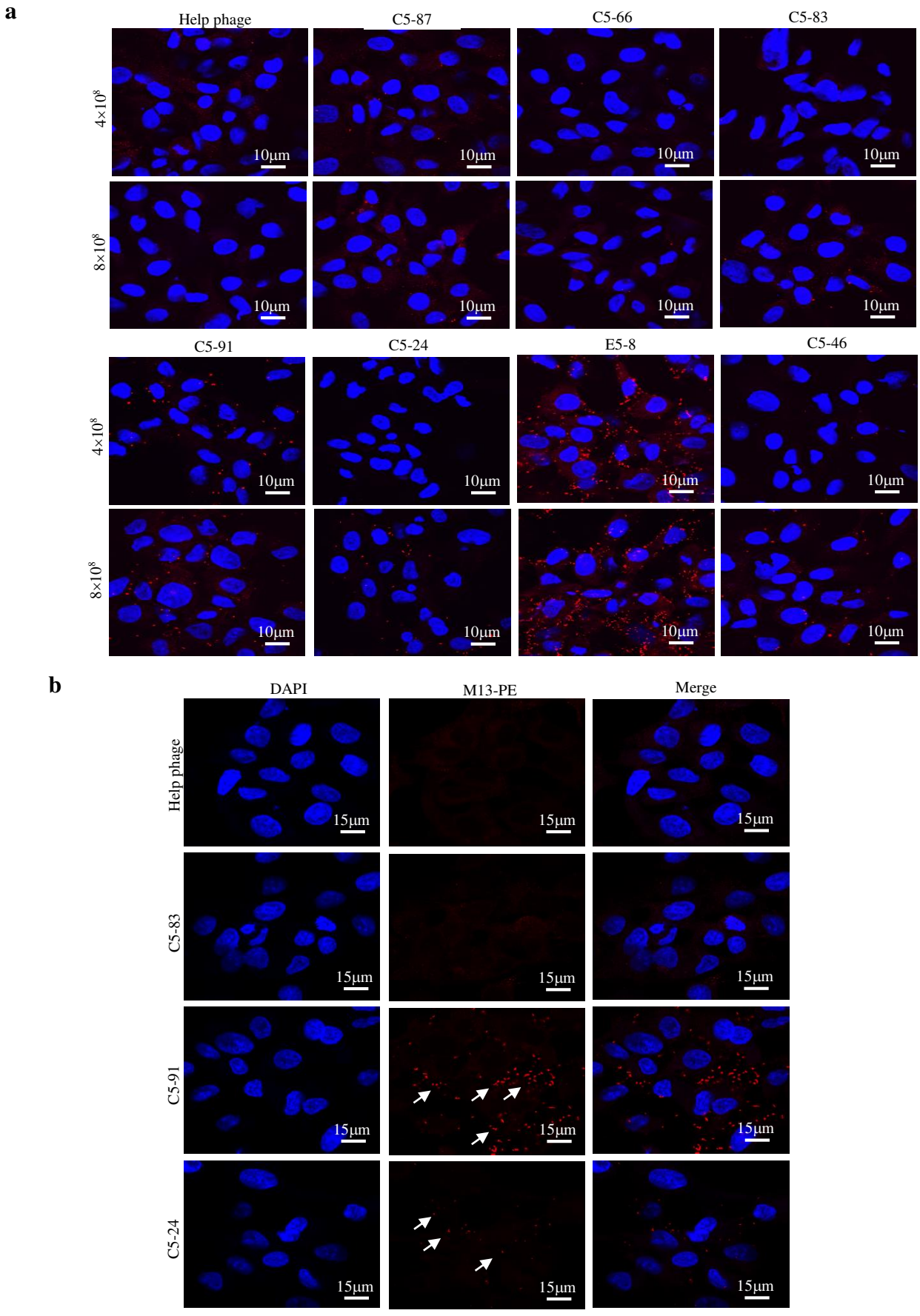

Fig. S3. Immunocytofluorescence of human chondrocyte cell line to validate the binding ability of the OA targeting phage clones. (a) Representative immunostaining for the binding activities of selected phage clones to the hPi-GL chondrocyte cell line in a dose-dependent manner (phage titers: 4×10^8 pfu/μl and $8 \times$

10^8 pfu/μl). **(b)** Representative immunostaining for the binding activities of selected phage clones (phage titer: 10^9 pfu/μl) to the hPi-GL chondrocyte cell line. Hochest 33342 was used for nuclear staining. Arrows indicate the fluorescent peptides binding targets.

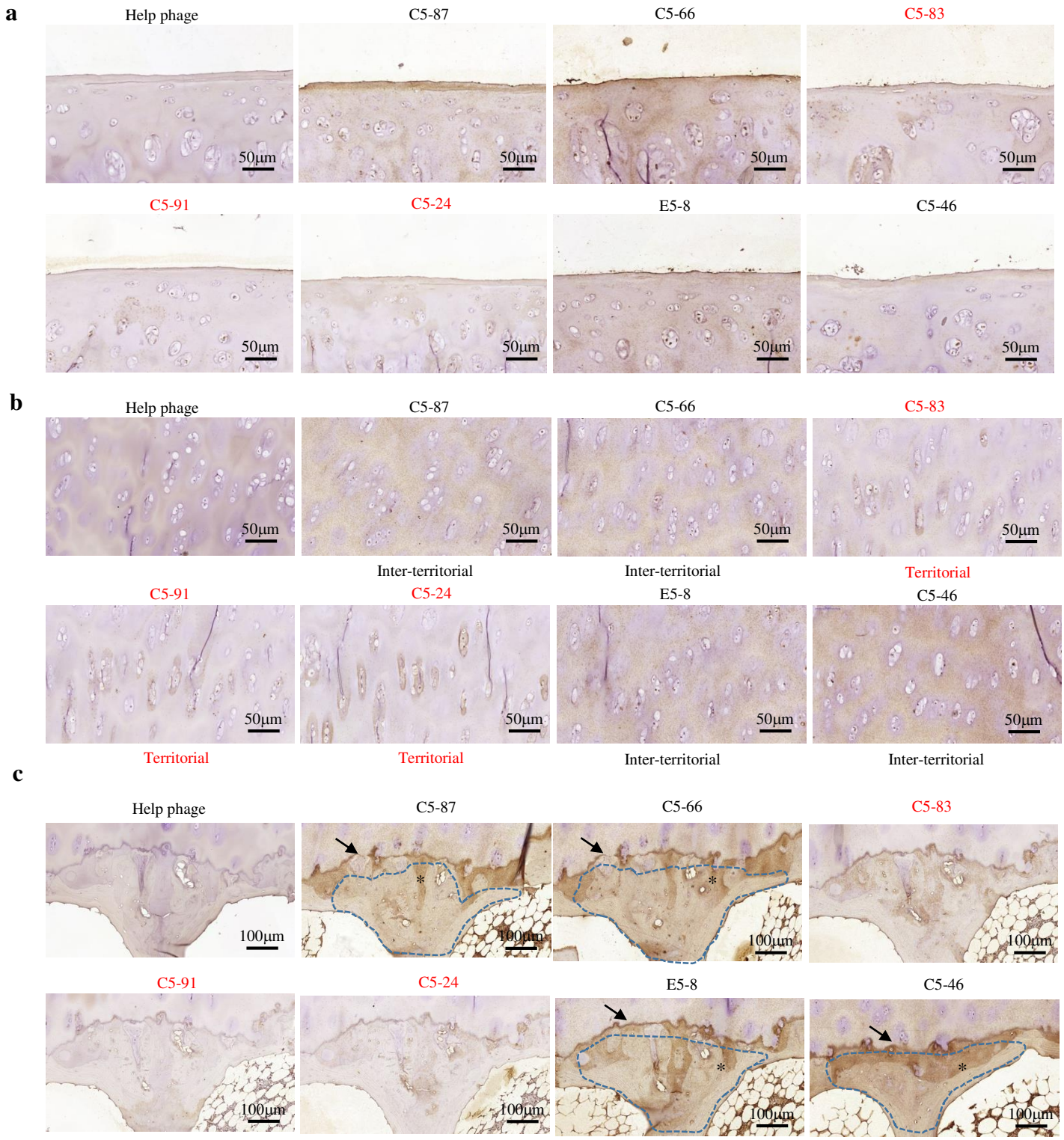

Fig. S4. Immunohistochemical staining to verify the human OA cartilage-targeting specificity of selected phage clones in human OA cartilage, synovium and meniscus. (a) Selected phage clones bound to hyaline cartilage exhibiting better signals than a helper phage clone. **(b)** C5-24, C5-83 and C5-91 bound to the territorial region of chondrocyte. **(c)** C5-24, C5-83 and C5-91 did not bind to tidemark (arrow), calcified cartilage (*) and subchondral trabecula (dotted circle).

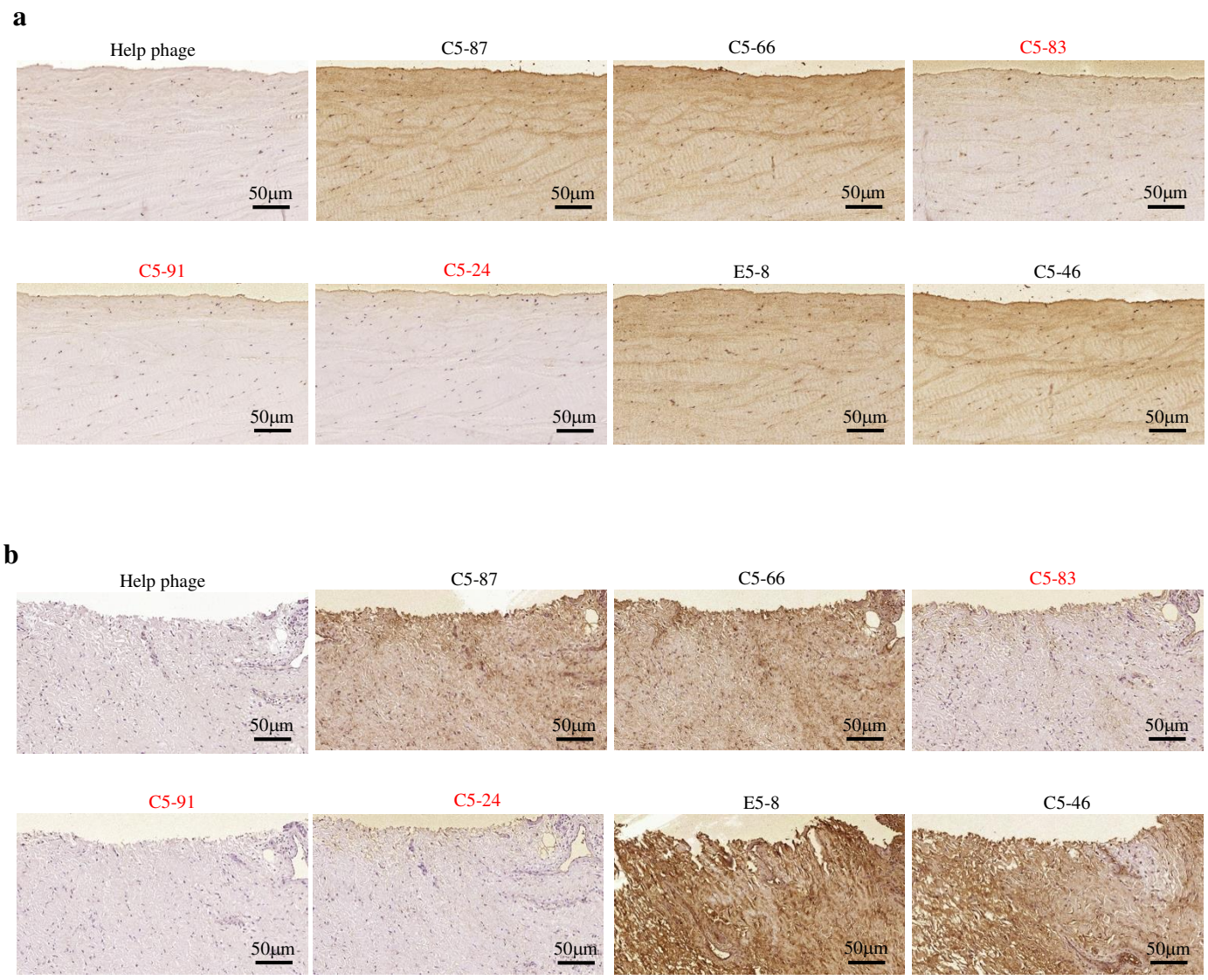

Fig. S5. **(a)** C5-24, C5-83 and C5-91 did not bind to meniscus tissues. **(b)** C5-24, C5-83 and C5-91 did not bind to synovium tissues. The same phage titer (5×10^8 pfu/μl) was used for each type of tissue. A helper phage was used as a negative control.

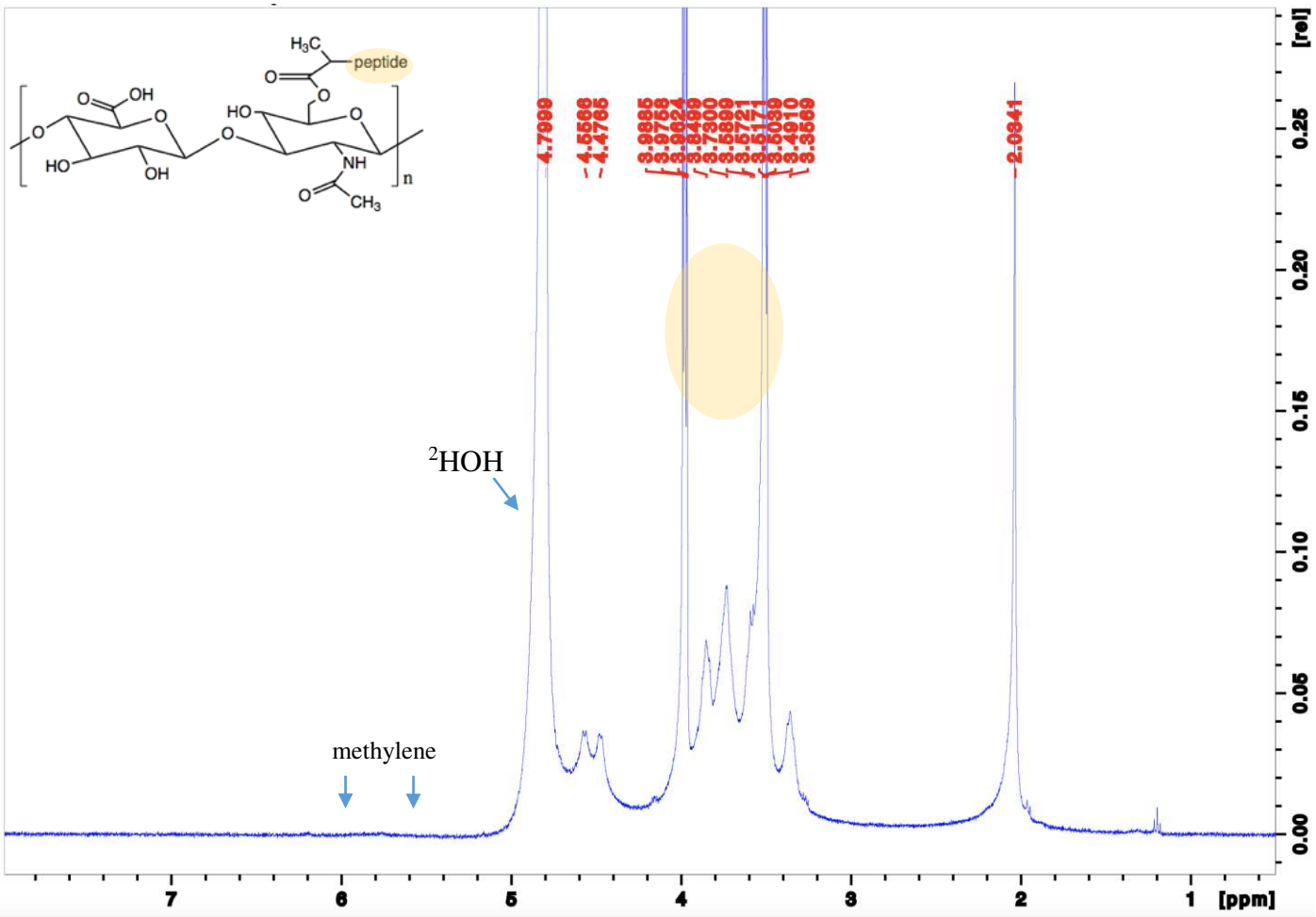

Fig. S6. ^{1}H proton-NMR analysis of scrambled peptide conjugated HA. The scrambled peptide modified HA was dissolved in D_2O and examined by ^{1}H-NMR identical to C5-24 peptide modified HA, with the ^{2}HOH peak at 4.8 ppm used as the reference line. The proton-NMR of peptide modified HA revealed extinguished methylene (6.0 and 5.6 ppm) signals and distinct amide proton shifts (3.9, 3.5 ppm) due to peptide crosslinking (thin yellow circle indicates the amide proton shifts).

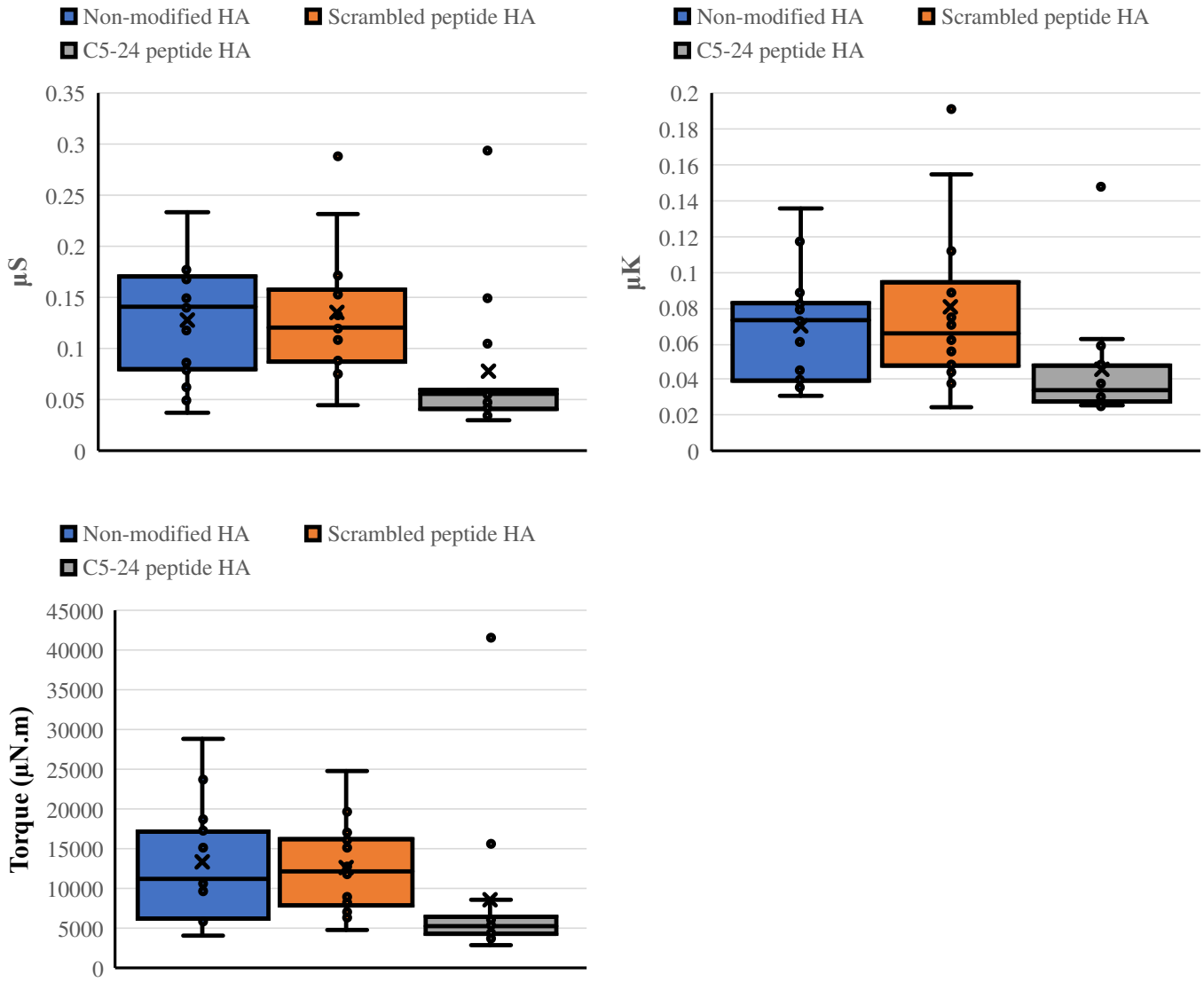

Fig. S7. Lubrication biomechanical testing in rheological pre-condition stage. Lubrication testing was performed in 14 stages. Although, the first two stages were considered negligible and used as a clearing or pre-shear stage. Data were similar to the following exact lubrication testing performed in stages 4-5, 7-8, 10-11 and 13-14. During each test, torque (τ) and axial force (N) were recorded for measurements of μk and μS.

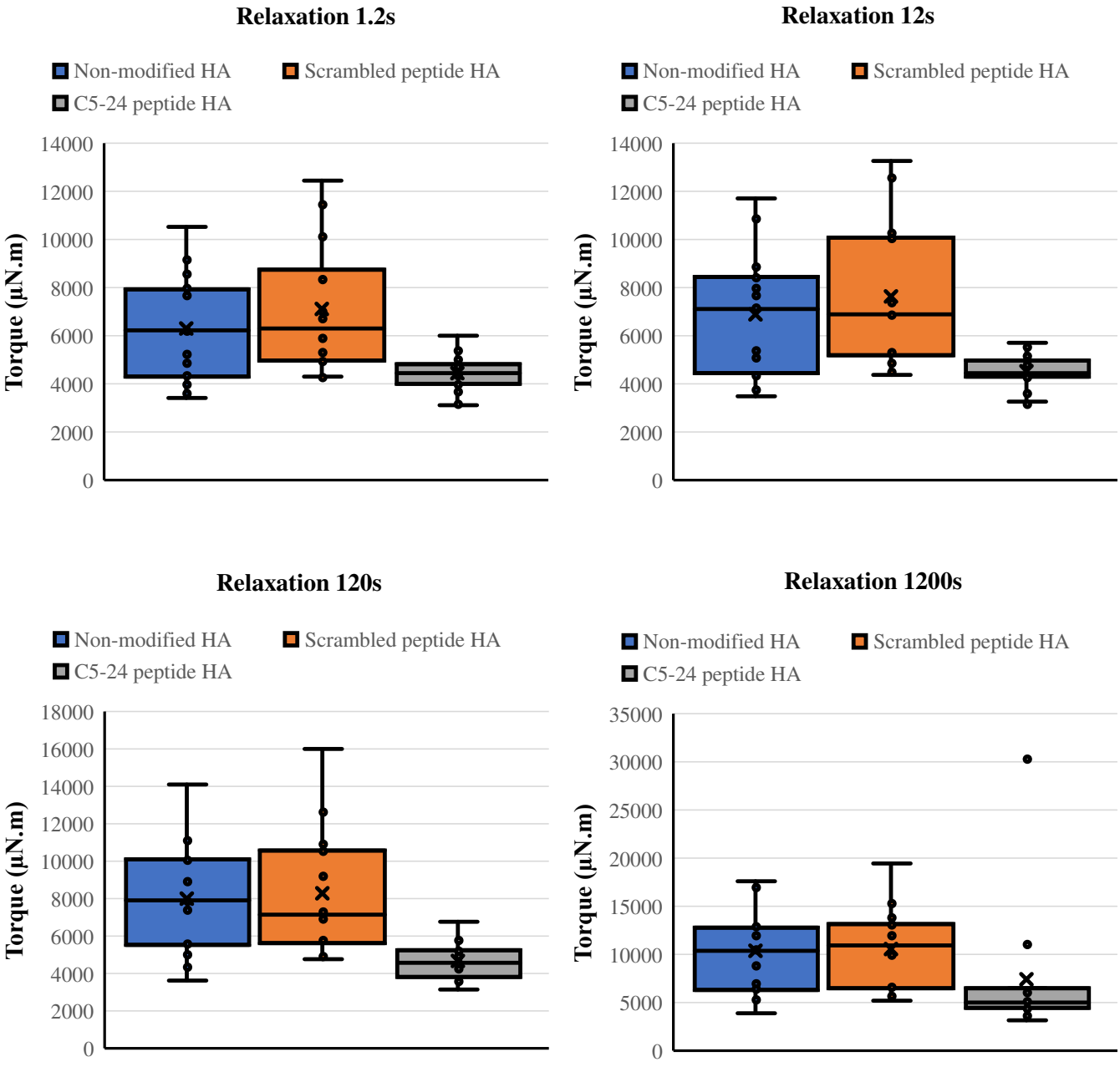

Fig. S8. Rheological torque measurement at post-relaxation. Rheological lubrication testing was performed in 14 stages. Samples were allowed to relax between tests for 1200, 120, 12 and 1.2 seconds to analyze the effect of different durations of relaxation, and the relaxation durations were set at stages 3, 6, 9 and 12, respectively. Lubrication data were recorded during stages 4-5, 7-8, 10-11 and 13-14; each stage was in a different direction of rotation and at a constant shear rate. During each test, torque (τ) and axial force (N) were recorded precisely.

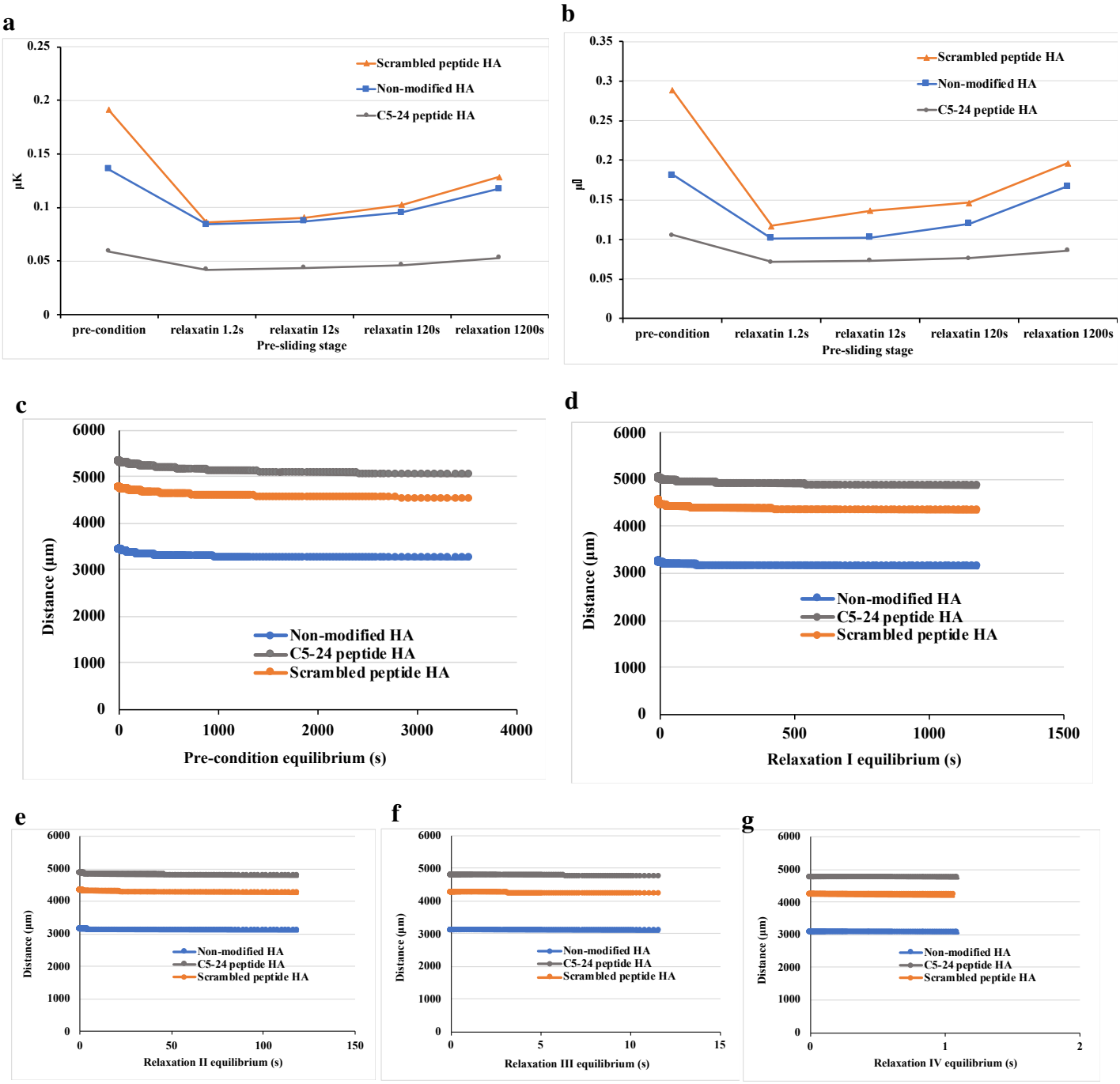

Fig. S9. Peptide modified HA served as lubricant to OA cartilage. Lubrication rheology analysis of respective OA cartilage retrieved from a clinical OA patient. **(a)** Dynamic friction. **(b)** Static friction. **(c)** Disc gap variance in pre-condition equilibrium 3600 second. **(d)** Disc gap variance in relaxation equilibrium I, 1200 second. **(e)** Disc gap variance in relaxation equilibrium II, 120 second. **(f)** Disc gap variance in relaxation equilibrium III, 12 second. **(g)** Disc gap variance in relaxation equilibrium IV, 1.2 second. Patient #1: Female, 72 years old, IRB number: CMUH108-REC1-046.

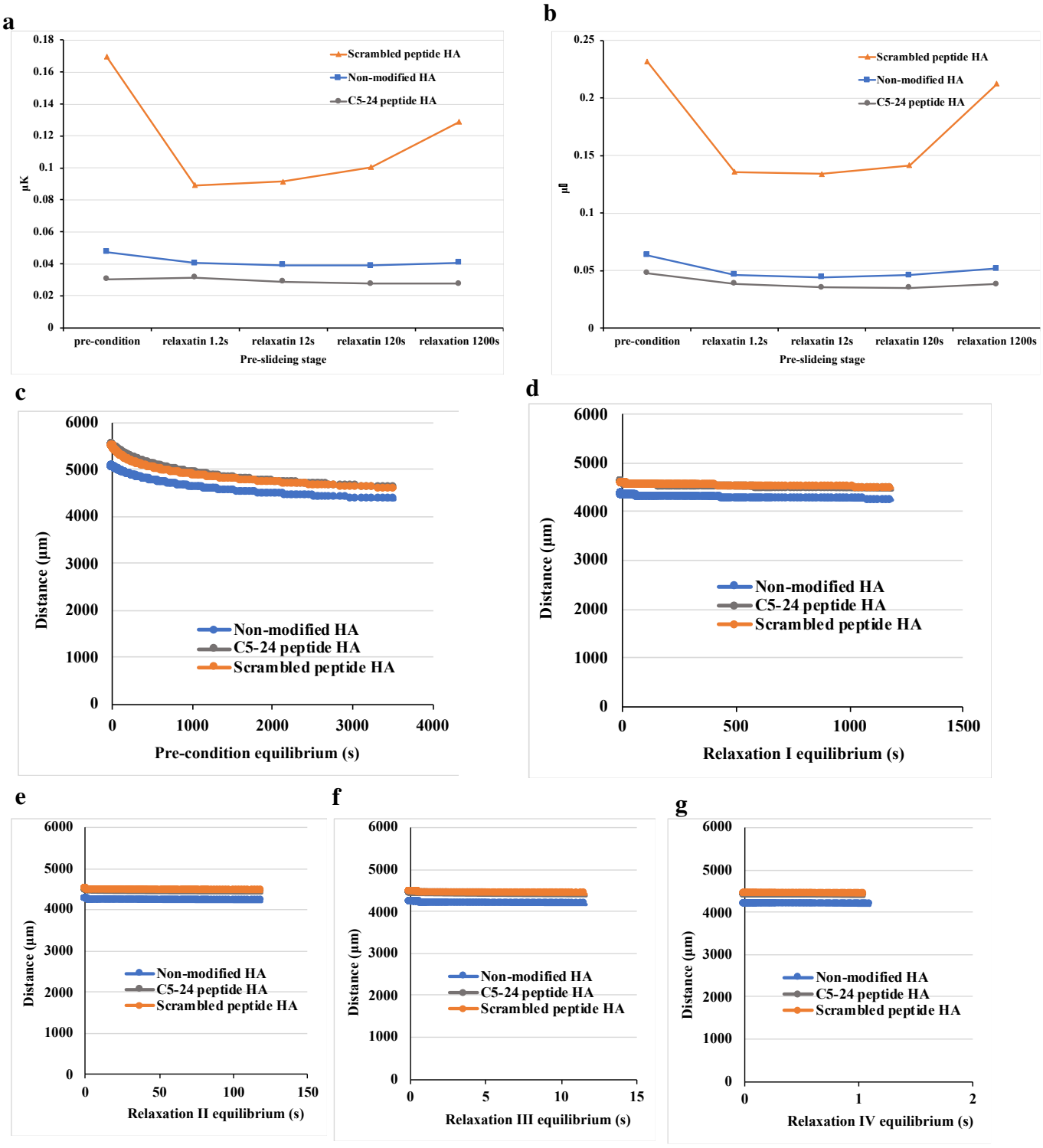

Fig. S10. Peptide modified HA served as lubricant to OA cartilage. Lubrication rheology analysis of respective OA cartilage retrieved from a clinical OA patient. **(a)** Dynamic friction. **(b)** Static friction. **(c)** Disc gap variance in pre-condition equilibrium 3600 second. **(d)** Disc gap variance in relaxation equilibrium I, 1200 second. **(e)** Disc gap variance in relaxation equilibrium II, 120 second. **(f)** Disc gap variance in relaxation equilibrium III, 12 second. **(g)** Disc gap variance in relaxation equilibrium IV, 1.2 second. Patient #2: Male, 63 years old. IRB number: CMUH108-REC1-046.

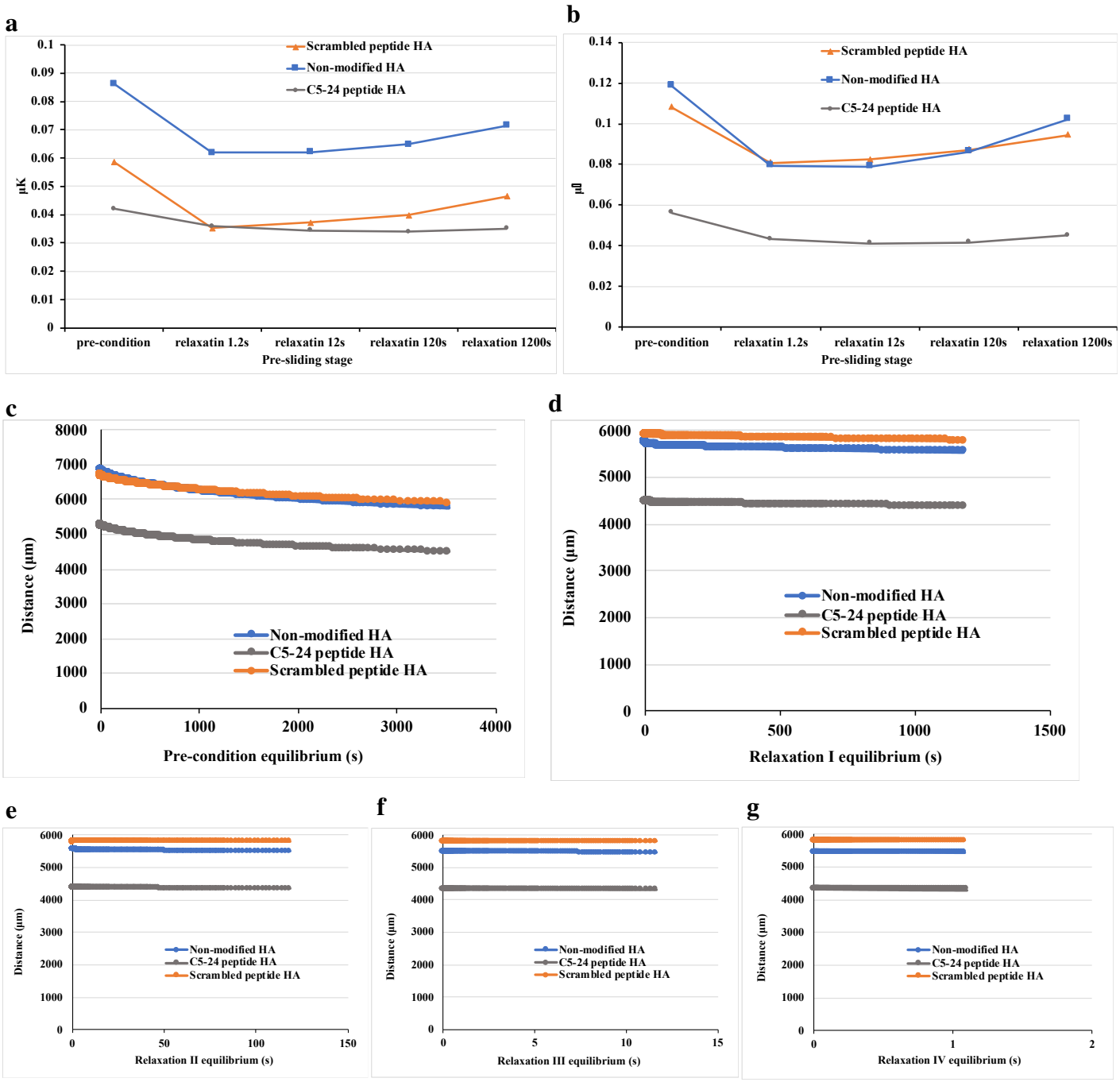

Fig. S11. Peptide modified HA served as lubricant to OA cartilage. Lubrication rheology analysis of respective OA cartilage retrieved from a clinical OA patient. **(a)** Dynamic friction. **(b)** Static friction. **(c)** Disc gap variance in pre-condition equilibrium 3600 second. **(d)** Disc gap variance in relaxation equilibrium I, 1200 second. **(e)** Disc gap variance in relaxation equilibrium II, 120 second. **(f)** Disc gap variance in relaxation equilibrium III, 12 second. **(g)** Disc gap variance in relaxation equilibrium IV, 1.2 second. Patient #3: Female, 68 years old. IRB number: CMUH108-REC1-046.

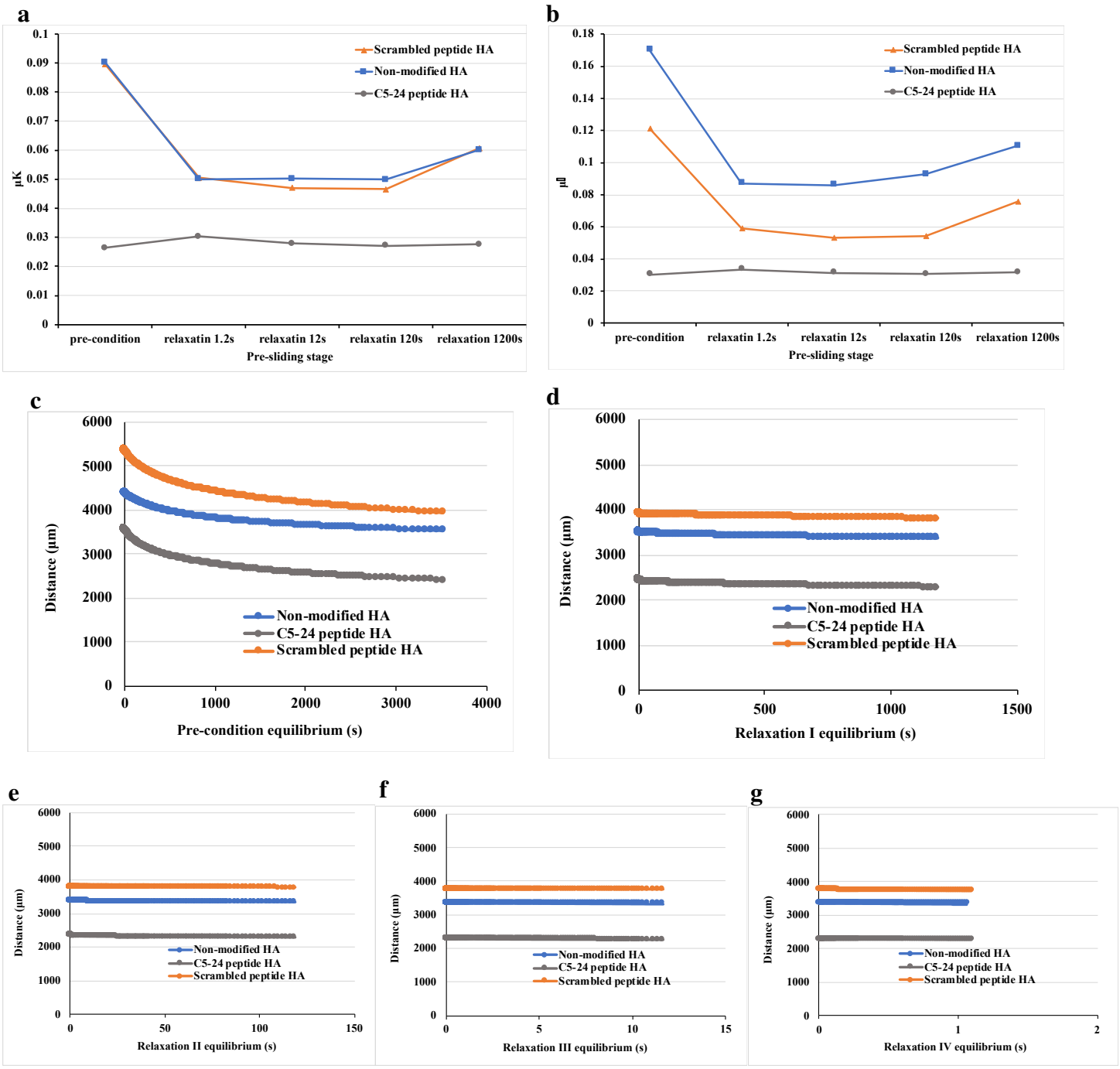

Fig. S12. Peptide modified HA served as lubricant to OA cartilage. Lubrication rheology analysis of respective OA cartilage retrieved from a clinical OA patient. **(a)** Dynamic friction. **(b)** Static friction. **(c)** Disc gap variance in pre-condition equilibrium 3600 second. **(d)** Disc gap variance in relaxation equilibrium I, 1200 second. **(e)** Disc gap variance in relaxation equilibrium II, 120 second. **(f)** Disc gap variance in relaxation equilibrium III, 12 second. **(g)** Disc gap variance in relaxation equilibrium IV, 1.2 second. Patient #4: Female, 78 years old. IRB number: CMUH108-REC1-046.

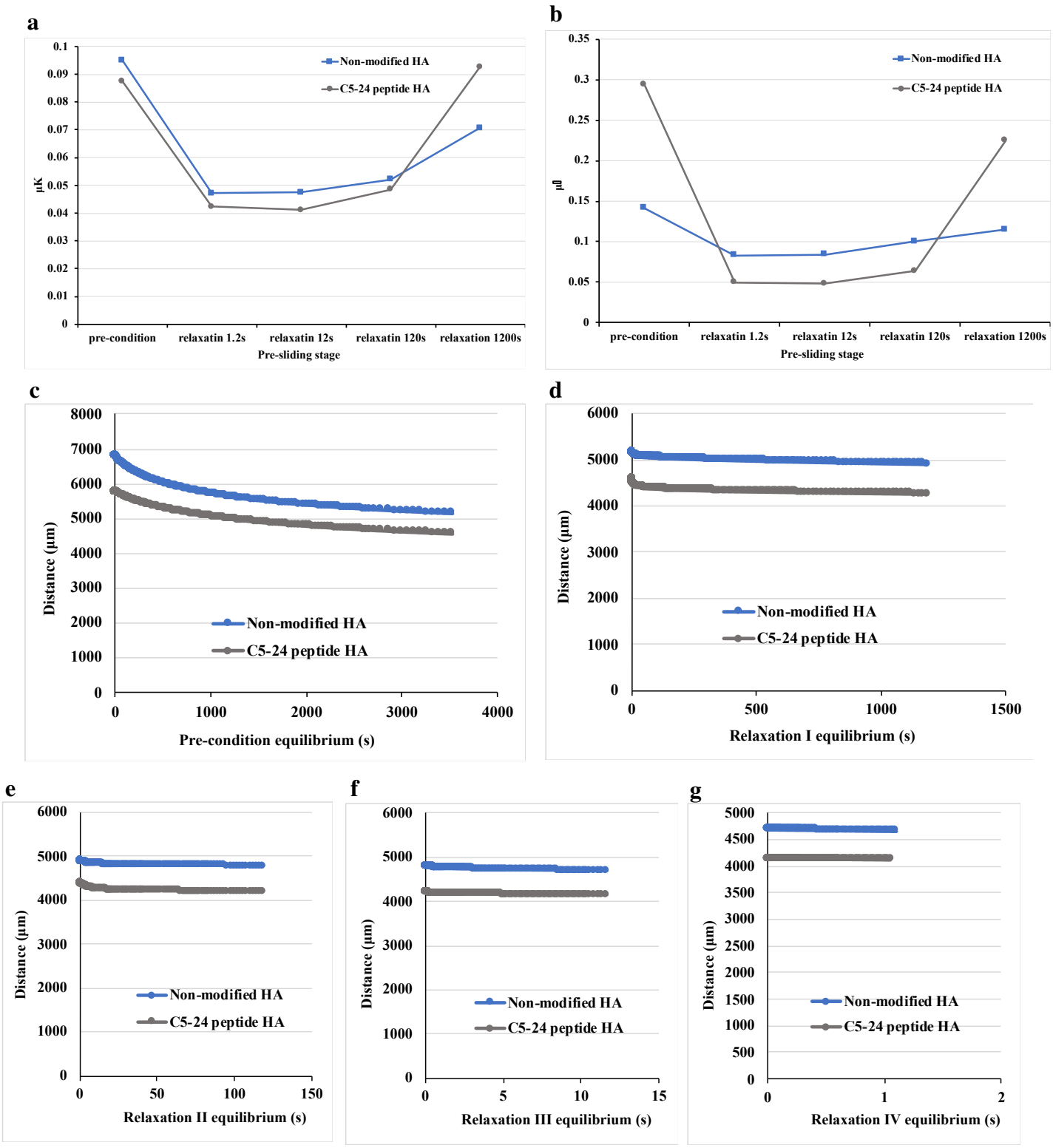

Fig. S13. Peptide modified HA served as lubricant to OA cartilage. Lubrication rheology analysis of respective OA cartilage retrieved from a clinical OA patient. **(a)** Dynamic friction. **(b)** Static friction. **(c)** Disc gap variance in pre-condition equilibrium 3600 second. **(d)** Disc gap variance in relaxation equilibrium I, 1200 second. **(e)** Disc gap variance in relaxation equilibrium II, 120 second. **(f)** Disc gap variance in relaxation equilibrium III, 12 second. **(g)** Disc gap variance in relaxation equilibrium IV, 1.2 second. Patient #9: Female, 53 years old. IRB number: CMUH108-REC1-046.

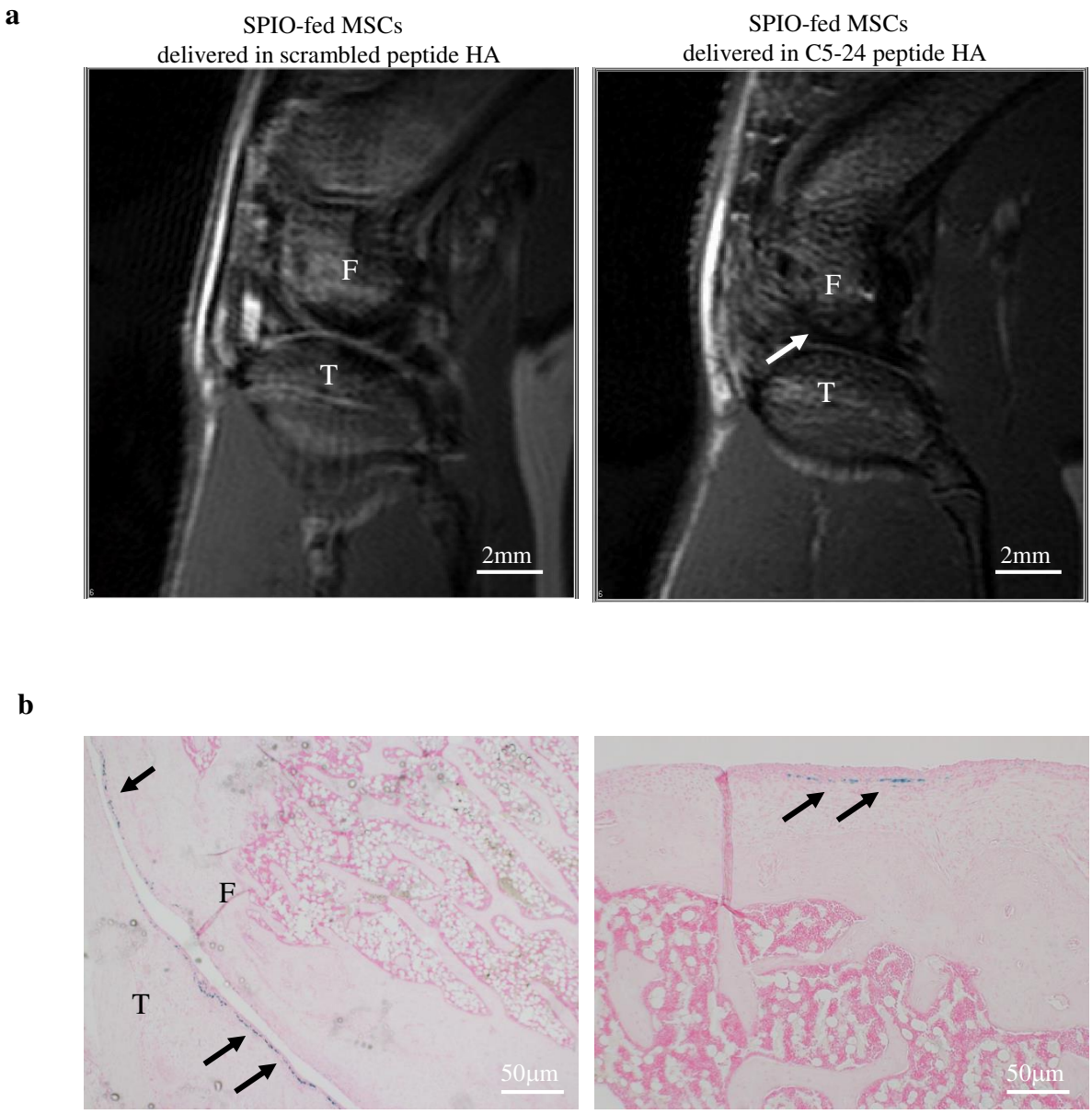

Fig. S14. MRI analysis and prussian blue staining for MSC tracking. **(a)** T1-weighted MRI detection (arrow indicates MRI reduction signal reflecting the presence of SPIO particles) and **(b)** Prussian blue staining of SPIO-labeled MSCs delivered in C5-24 peptide-conjugated HA at post-transplantation day 3 in rat OA joint. F: distal femoral end; T: proximal tibial end. (arrows indicate the Prussian blue staining signals).

a

Title	Accession	Identity	Sequence Length	Alignment Length	Bit Score	E-Value	Positive	Resolution	SCOPE
Chain A, Fragment Of Human Fibronectin Encompassing Type-Iii Repeats 7 Through 10	1FNF_A	30	368	377	133.265	1.18E-32	48	2	b.1.2.1
Chain A, N-Terminal Nc4 Domain Of Collagen Ix	2UUR_A	31	245	219	117.087	2.71E-28	50	1.8	
Chain A, Structure of the four-domain fragment Fn7B89 of oncofetal fibronectin	3T1W_A	28	375	370	117.472	2.97E-27	48	2.4	
Chain A, Vla1 Rdeltah I-domain Complexed With A Quadruple Mutant Of The Aqc2 Fab >gi|99031850|pdb|2B2X|B Chain B, Vla1 Rdeltah I-domain Complexed With A Quadruple Mutant Of The Aqc2 Fab	2B2X_A	36	223	192	110.153	3.23E-26	56	2.2	c.62.1.1
Chain A, Crystal Structure Of Rat A1b1 Integrin I-Domain. >gi|7766812|pdb|1CK4|B Chain B, Crystal Structure Of Rat A1b1 Integrin I-Domain.	1CK4_A	36	198	186	108.612	6.56E-26	55	2.2	c.62.1.1
Chain A, Crystal Structure Of A Chimeric Alpha1 Integrin I-Domain In Complex With The Fab Fragment Of A Humanized Neutralizing Antibody >gi|30749472|pdb|1MHP|B Chain B, Crystal Structure Of A Chimeric Alpha1 Integrin I-Domain In Complex With The Fab Fragment Of A Humanized Neutralizing Antibody	1MHP_A	36	192	182	107.842	8.42E-26	56	2.8	c.62.1.1
Chain A, Structure of integrin alpha1beta1 and alpha2beta1 I-domains explain differential calcium-mediated ligand recognition >gi|1177806036|pdb|5HGJ|B Chain B, Structure of integrin alpha1beta1 and alpha2beta1 I-domains explain differential calcium-mediated ligand recognition	5HGJ_A	37	195	182	107.842	1.21E-25	56	1.399	
Chain B, I Domain From Integrin Alpha1-beta1	1QC5_B	37	192	186	107.071	1.64E-25	55	2	c.62.1.1
Chain A, Integrin alpha-1	2M32_A	37	192	186	107.071	1.80E-25	55		
Chain A, Activated Conformation Of Integrin Alpha1 I-Domain Mutant >gi|354459830|pdb|4A0Q|B Chain B, Activated Conformation Of Integrin Alpha1 I-Domain Mutant	4A0Q_A	36	201	186	105.531	8.51E-25	55	1.9	c.62.1.1

b

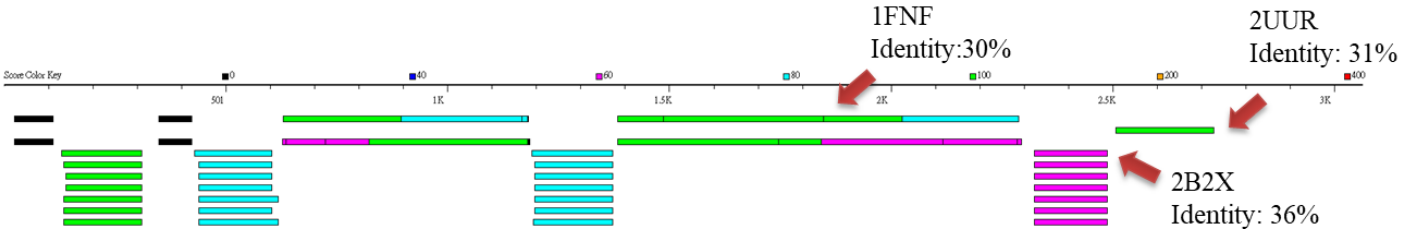

Fig. S15. Homology alignment of human Collagen XII for homology model establishment. (a) BLAST results of sequence alignment with the top 10 aligned template candidates. **(b)** Human Collagen XII sequence map aligned with the top 10 paired template candidates, subsequently three different aligned parts with PDB code: 1FNF, 2B2X and 2UUR were used for homology model reconstruction.

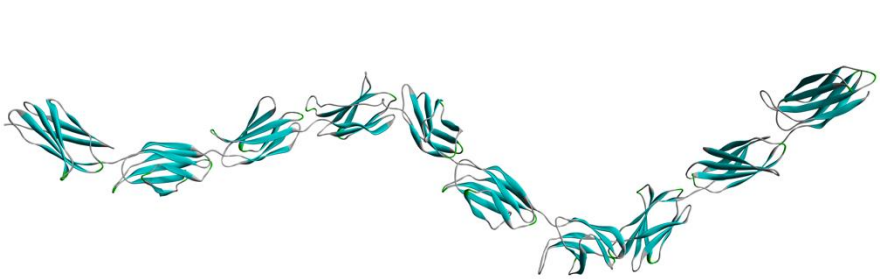

Collagen XII L1385~S2295
template, with 1FNF identity 30%

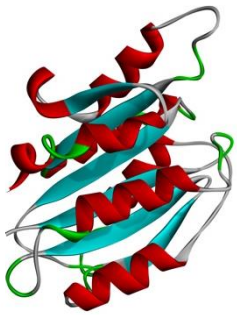

Collagen XII
K2321~L2513
template, with 2B2X
identity 36%

Collagen XII
S2506~P2724
template, with
2UUR identity 31%

	Verify Score	Verify Expected High Score	Verify Expected Low Score	DOPE Score	PDF Total Energy
Collagen XII-1FNF L1385~S2295	337.96	418.24	188.21	-80718.94	5933.06
Collagen XII-2B2X K2321~L2513	56.66	87.51	39.38	-20006.98	938.29
Collagen XII-2UUR S2506~P2724	87.72	99.40	44.73	-23264.95	698.74

Fig. S16. Establishment of human Collagen XII homology model and validation. Three different parts of human Collagen XII homology models were built using MODELER based on the templates (PDB code: 1FNF, 2B2X, 2UUR) from BLAST result. The negative DOPE score and verify score which was close to the expected high score for each model indicated the qualified theoretical model.

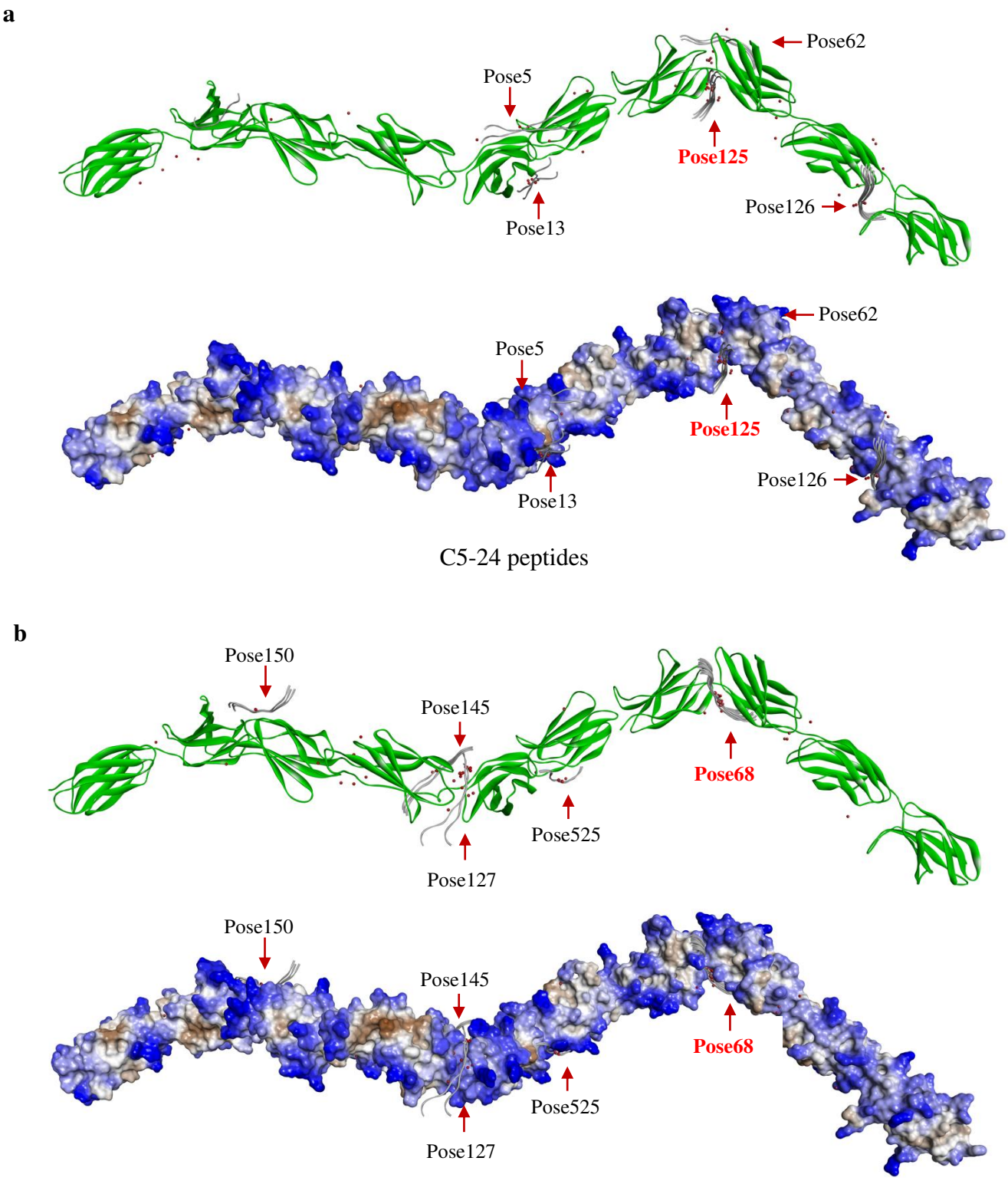

Fig. S17. Predicted docking sites of C5-24 and C5-91 peptides to human Collagen XII. **(a)** Predicted docking sites of C5-24 peptides in Collagen XII L1385~S2295 template, protein structure is showed in cartoon and surface representation, respectively. **(b)** Predicted docking sites of C5-91 peptides in Collagen XII L1385~S2295 template. The docking poses of each peptide were presented as red spots. Pose 125 of C5-24 and Pose 68 of C5-91 located in the same binding region. Blue represent hydrophilic region, and brown represent hydrophobic region.

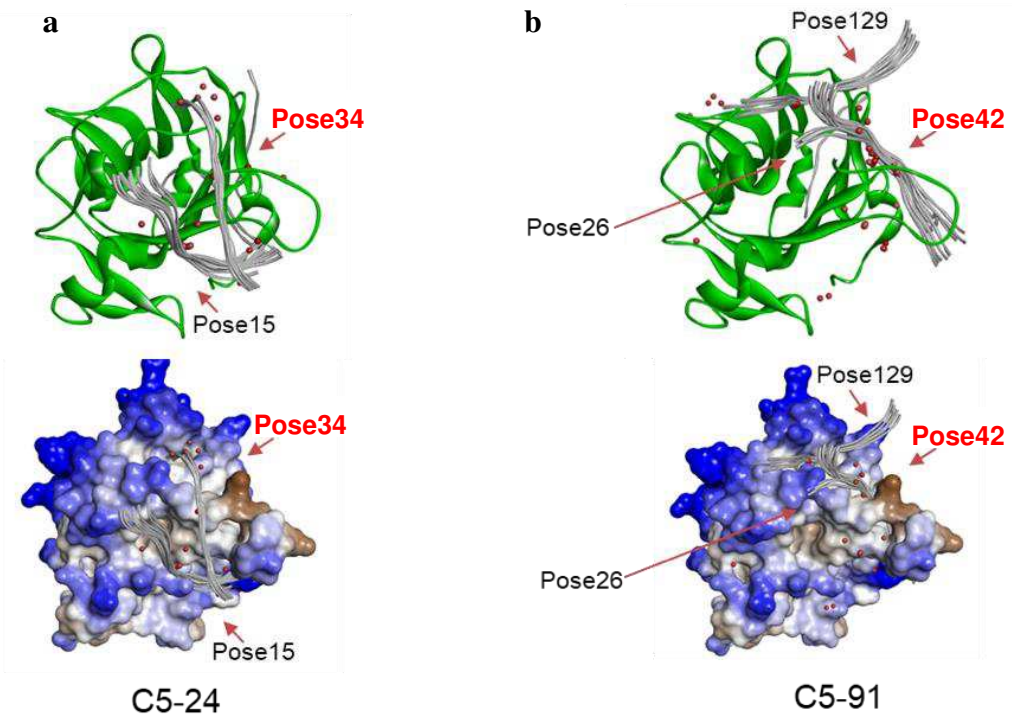

Fig. S18. Predicted docking sites of C5-24 and C5-91 peptides to human Collagen XII. Predicted docking sites of C5-24 and C5-91 peptides in Collagen XII C-terminus S2506~P2724 domain, protein structure is showed as cartoon and surface representation in upper and lower panels, respectively. The docking poses of each peptide were presented as red spots. Pose 34 of C5-24 **(a)** and Pose 42 of C5-91 **(b)** located in the same binding region. Blue represents hydrophilic region, and brown represents hydrophobic region.

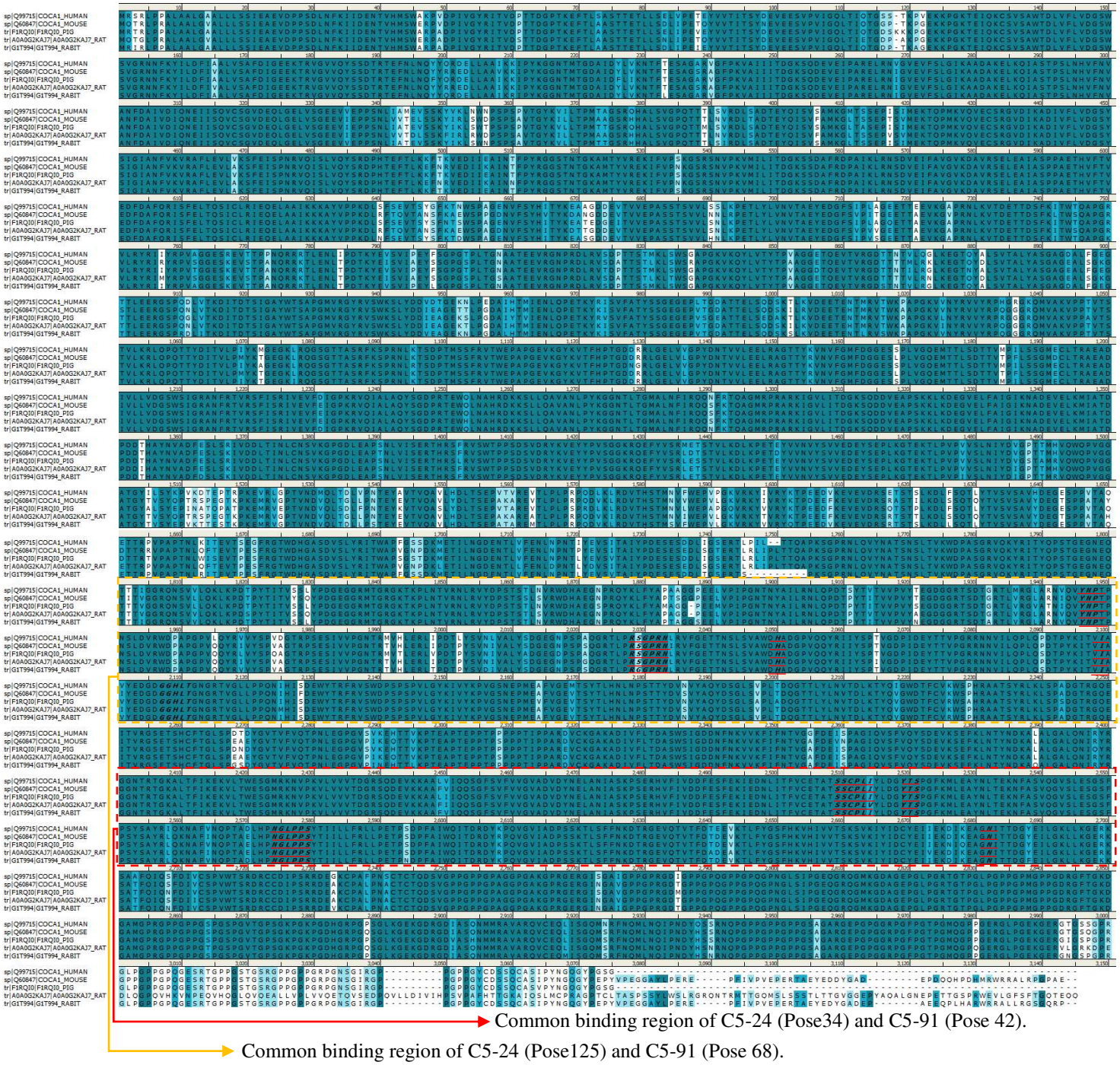

Fig. S19. Sequence alignment of Collagen XII chain in different animal species used in this study. The Human (Q99715), Mouse (Q60847), Pig (F1RQI0), Rat (A0A0G2KAJ7), and Rabbit (G1T994) sequences were retrieved from Uniprot database for analysis and showed high sequence similarity (90.3%) and identity (83.7%). Background color intensity represents the 100% identical (deepest) to completely non-related (white). The common binding regions of C5-24 and C5-91 peptides at the indicated pose are labeled with dotted line. The overlapped docking residues of C5-24 and C5-91 peptides to ColXII between these five species are showed in bold letters and underlined, which are highly conserved in five species.

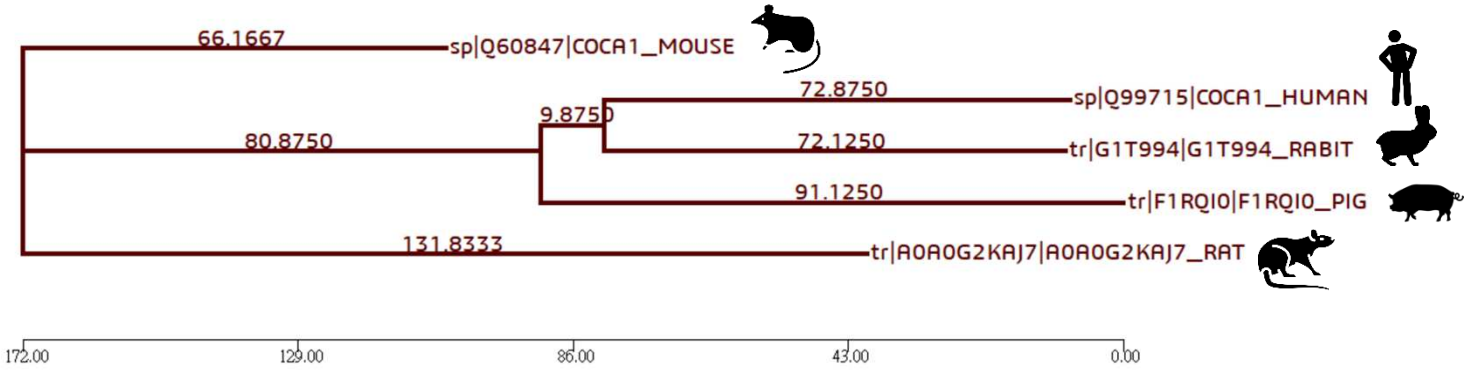

Fig. S20. Phylogenic tree of Collagen XII chain in different animal species. The Collagen XII sequence of Human (Q99715), Mouse (Q60847), Pig (F1RQI0), Rat (A0A0G2KAJ7), and Rabbit (G1T994) were retrieved from Uniprot database, and used to compare the similarity (90.3%) and identity (83.7%). The phylogenic analysis of Collagen XII between five species revealed that the species with correspondent degree to human from high to low are rabbit, pig, mouse and rat.

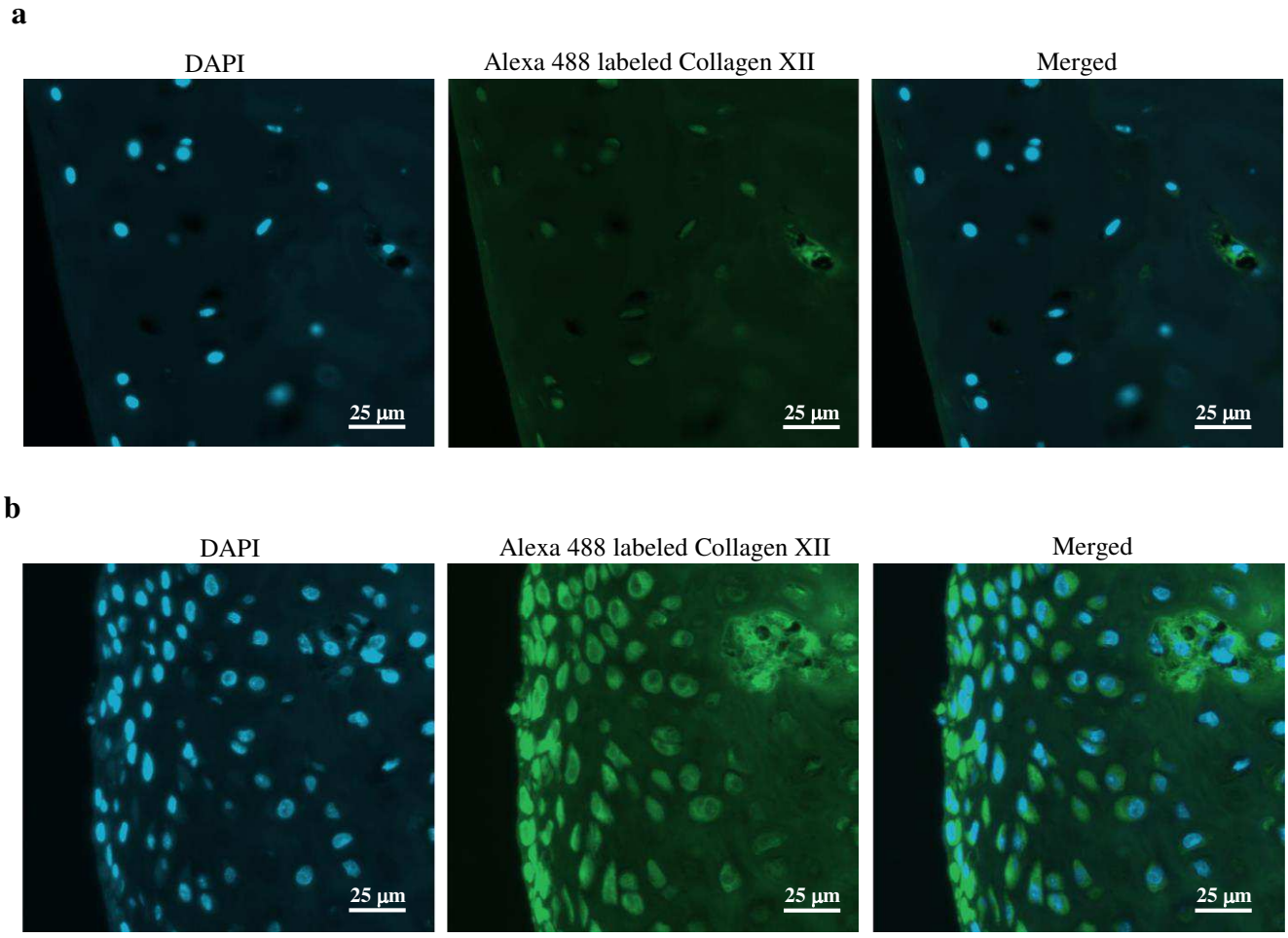

Fig. S21. Expression of collagen XII in rat normal and OA joints. Normal and enzyme-induced OA knee joints were subjected to immunofluorescence for collagen XII. **(a)** A representative image of normal articular cartilage shows a smooth surface and low expression of collagen XII. **(b)** A representative image of OA articular cartilage shows that the cartilage surface is broken and accompanied by a large amount of strong XII collagen expression in the territorial region.

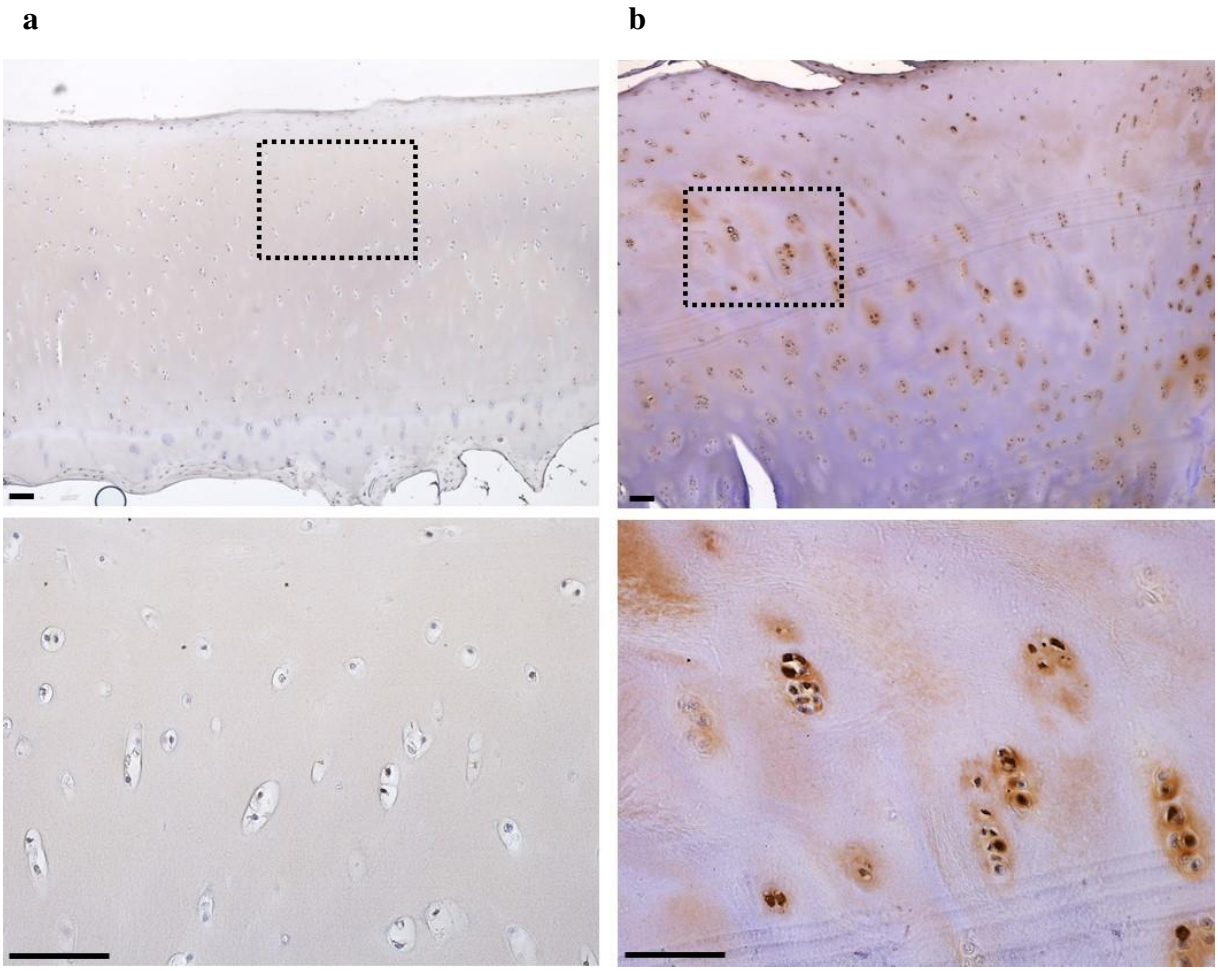

Fig. S22. Expression of collagen XII in human non-OA and OA joints. Non-OA and OA articular cartilages were subjected to immunohistochemistry for collagen XII. Expression of collagen XII is visualized as brown color (DAB). **(a)** A representative image of non-OA articular cartilage shows a smooth surface and low expression of collagen XII. **(b)** A representative image of OA articular cartilage shows that the cartilage surface is broken and accompanied by clusters of chondrocytes and a large amount of strong XII collagen expression in the territorial region. Non-OA cartilage was derived from a 23-year-old woman who underwent limb salvage procedure and signed the informed consent form. The rectangular frame in the upper panel is enlarged in the lower panel. Bar = 100 μm.

Table S1. Alignment of phage-displayed peptide sequences selected by biopanning of human cartilage tissue and chondrocyte-secreted protein (grouping according to motifs similarity).

	Phage clone	Amino acid sequence	Frequency
1	C5-3, C5-50, C5-84, C5-87	**GDYVIDWNFIEW**	4/24
	C5-37	**TVGSFFVEWMMH**	1/24
	C5-66	**DIGGWFVEWSLA**	1/24
2	C5-22, C5-83, C5-92	**DWGYFSWAYDSA**	3/24
	C5-43	**DWYTVSWLTDSN**	1/24
3	C5-42, C5-91	**DAYWHPVWVHDP**	2/24
	C5-24	**DLQYWYPIWDTH**	1/24
	C5-12	**HVYQKPSYWWYP**	1/24
	C5-21	**TWHFVDFSADTH**	1/24
4	E5-8, E5-48	**DYFTLDFTFDSW**	2/24
	C5-46	**NQVYFHYFDLDF**	1/24
5	E4-14, E5-24	**SPWWLWKAHNEA**	2/24
6	C5-38	**EVFNHYIQYSTE**	1/24
7	E4-1	**LPGMELFWNVAN**	1/24
8	E4-4	**DTFVFGSSKWRA**	1/24
9	E4-15	**SNNMRAPVNEIY**	1/24

C: Phage clones targeting human cartilage tissue lysates.

E: Phage clones targeting human cartilage tissue pieces.

Table S2. Quantification of topological binding activities of each tested phage clone to human cartilage specimens. According to the paper, we classified IHC staining cells. The staining cells had more than 10% of cells and were scored as – (Non-detected), 1+, 2+, or 3+ according to the intensity and partial/complete staining (*8*). Therefore, we analyzed each phage stained-OA section such as surface, territorial, inter-territorial, tidemark, calcified cartilage, and trabecula. Besides, we also analyzed meniscus and synovium.

	C5-87	C5-66	C5-83	C5-91	C5-24	E5-8	C5-46
Surface	++	+++	+	+	+	++	+
Territorial	-	-	+	+	+++	-	-
Inter-territorial	+++	+++	++	+	+	+++	+++
Tidemark	+++	+++	++	+	+	+++	+++
Calcified cartilage	+++	+++	++	+	+	+++	+++
Trabecula	+++	+++	++	+	+	+++	+++
Meniscus	+++	+++	++	-	-	+++	+++
Synovium	++	++	+	-	-	+++	++

Table S3. Target prediction. LC-MS/MS analysis of isolated C5-24-targeting proteins in human OA cartilage. The data were further subjected to algorithm searching on the basis of MASCOT software.

COIP-1		
name	mass	score
Basement membrane-specific heparan sulfate proteoglycan core protein	468532	87
Chondroitin sulfate proteoglycan 4	250382	110
Collagen alpha-1(XII) chain	332941	850
Collagen alpha-3(VI) chain	343457	372

COIP-3		
name	mass	score
Alpha-aminoadipic semialdehyde dehydrogenase	58450	133
Angiopoietin-related protein 2	57068	58
Anosmin-1	76064	202
ATP synthase subunit alpha, mitochondrial	59714	91
ATP synthase subunit beta, mitochondrial	56525	950

COIP-5		
name	mass	score
Lactadherin	46095	83
Matrilin-3	52783	756
Phosphoglycerate kinase 1	44586	1282
Pigment epithelium-derived factor	46283	278
Procollagen C-endopeptidase enhancer 2	45687	1002
Prolargin	43782	107
Protein NDRG1	42808	71
Putative elongation factor 1-alpha-like 3	50153	96
Pyruvate kinase PKM	57900	230
Serine protease HTRA1	51255	120
Sushi repeat-containing protein SRPX	51538	79
Sushi repeat-containing protein SRPX2	52938	305
Vimentin	53619	306

Figures

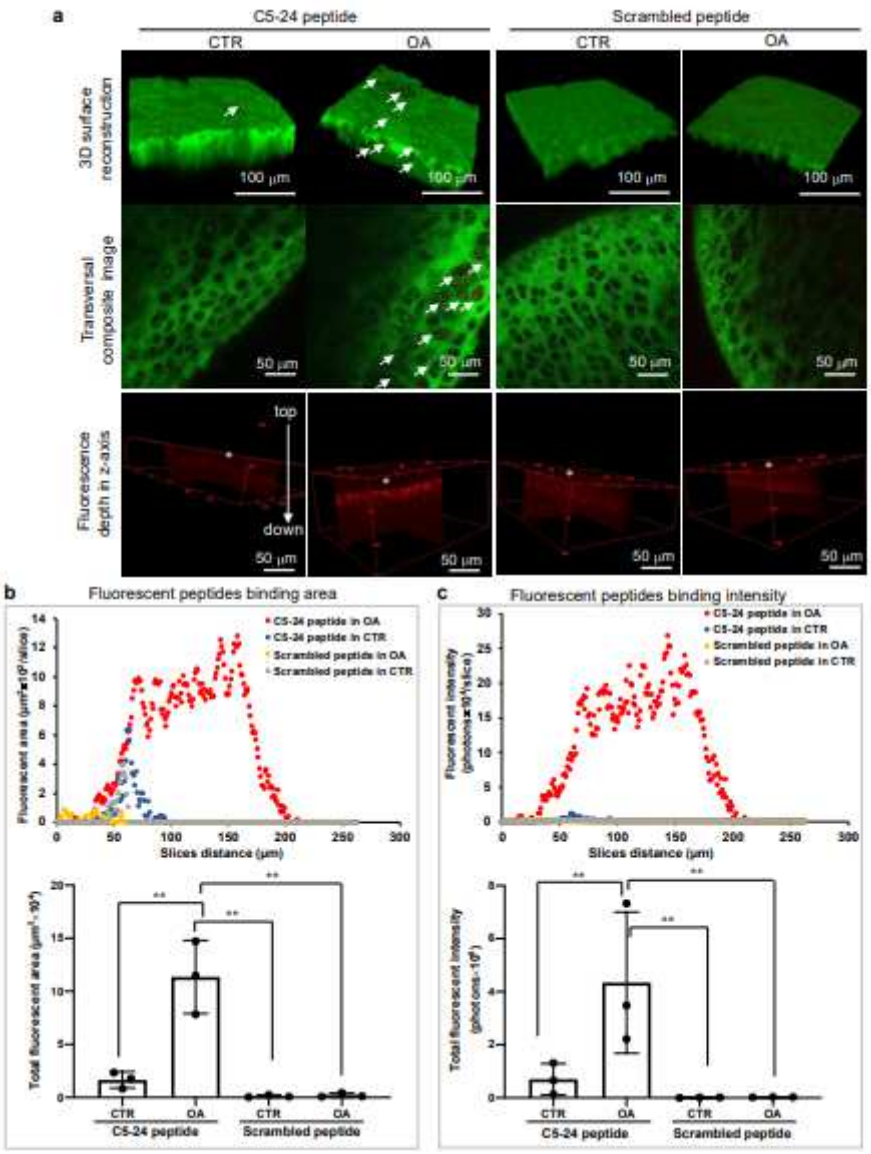

Figure 1

[Please see the manuscript file to view the figure caption.]

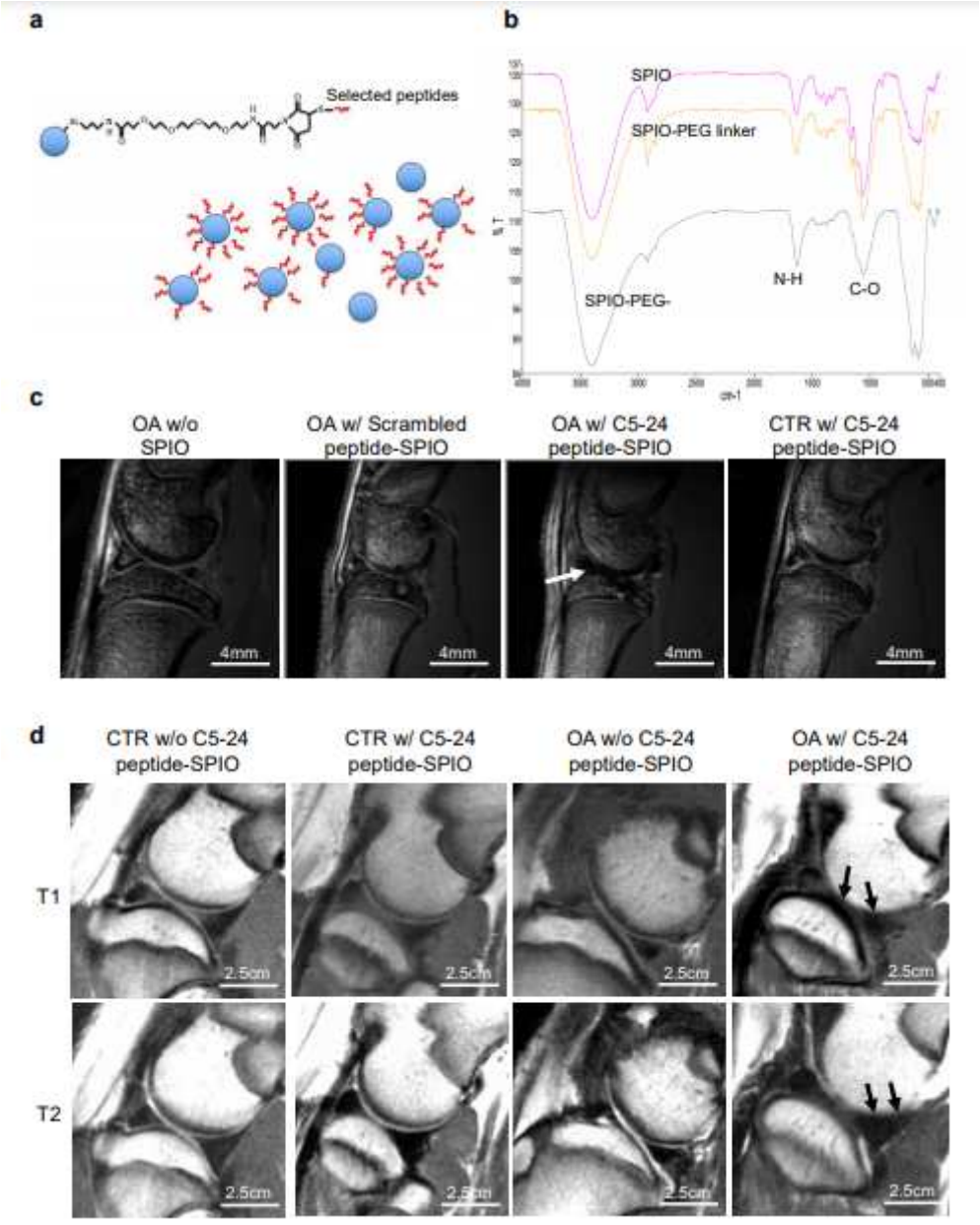

Figure 2

[Please see the manuscript file to view the figure caption.]

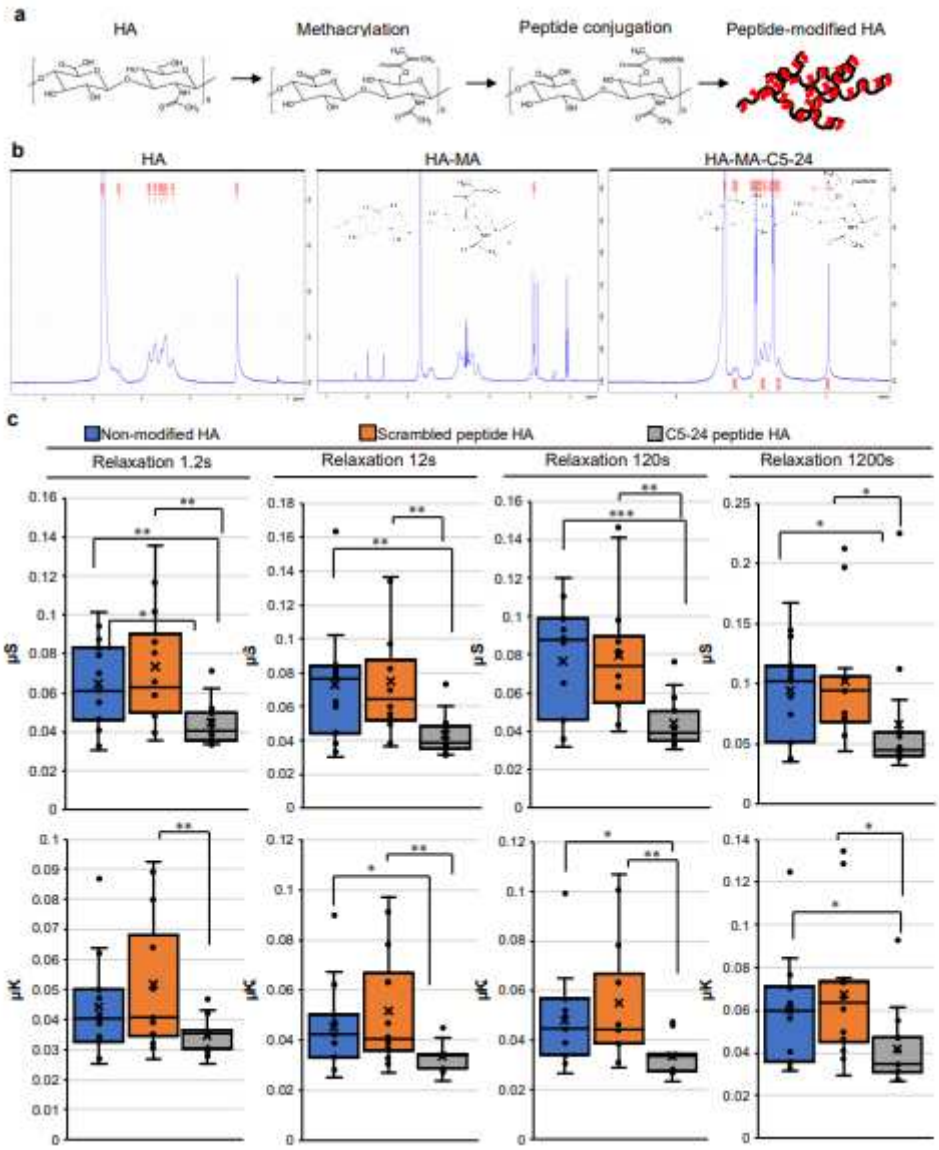

Figure 3

[Please see the manuscript file to view the figure caption.]

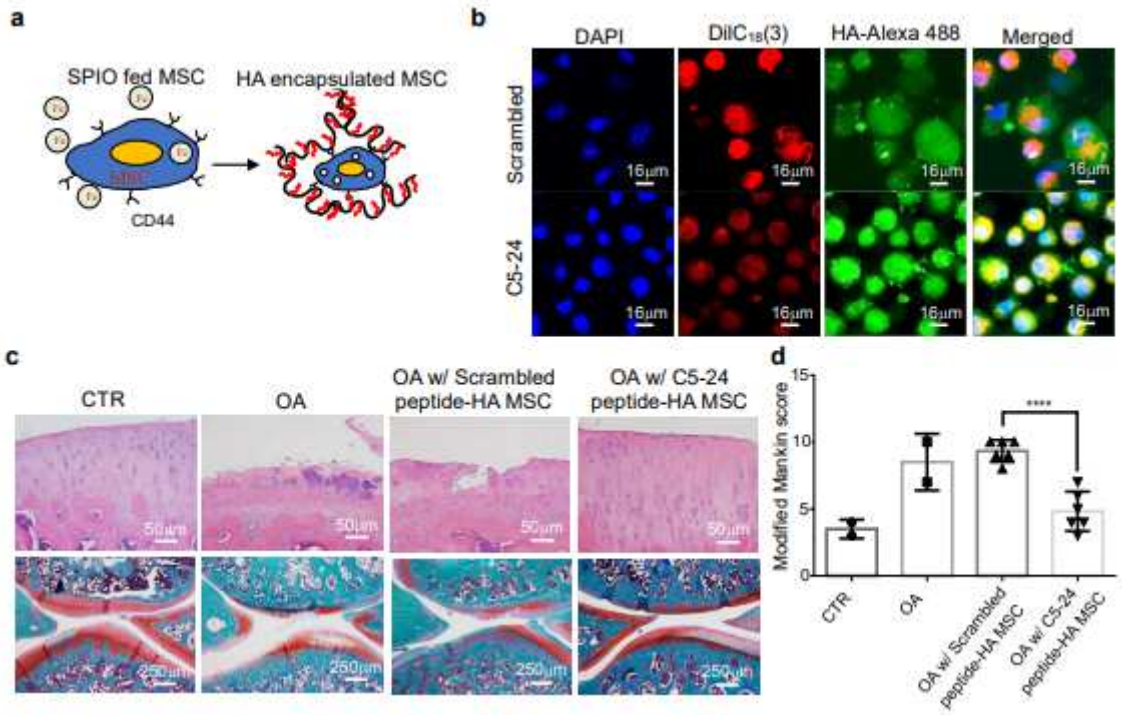

Figure 4

[Please see the manuscript file to view the figure caption.]

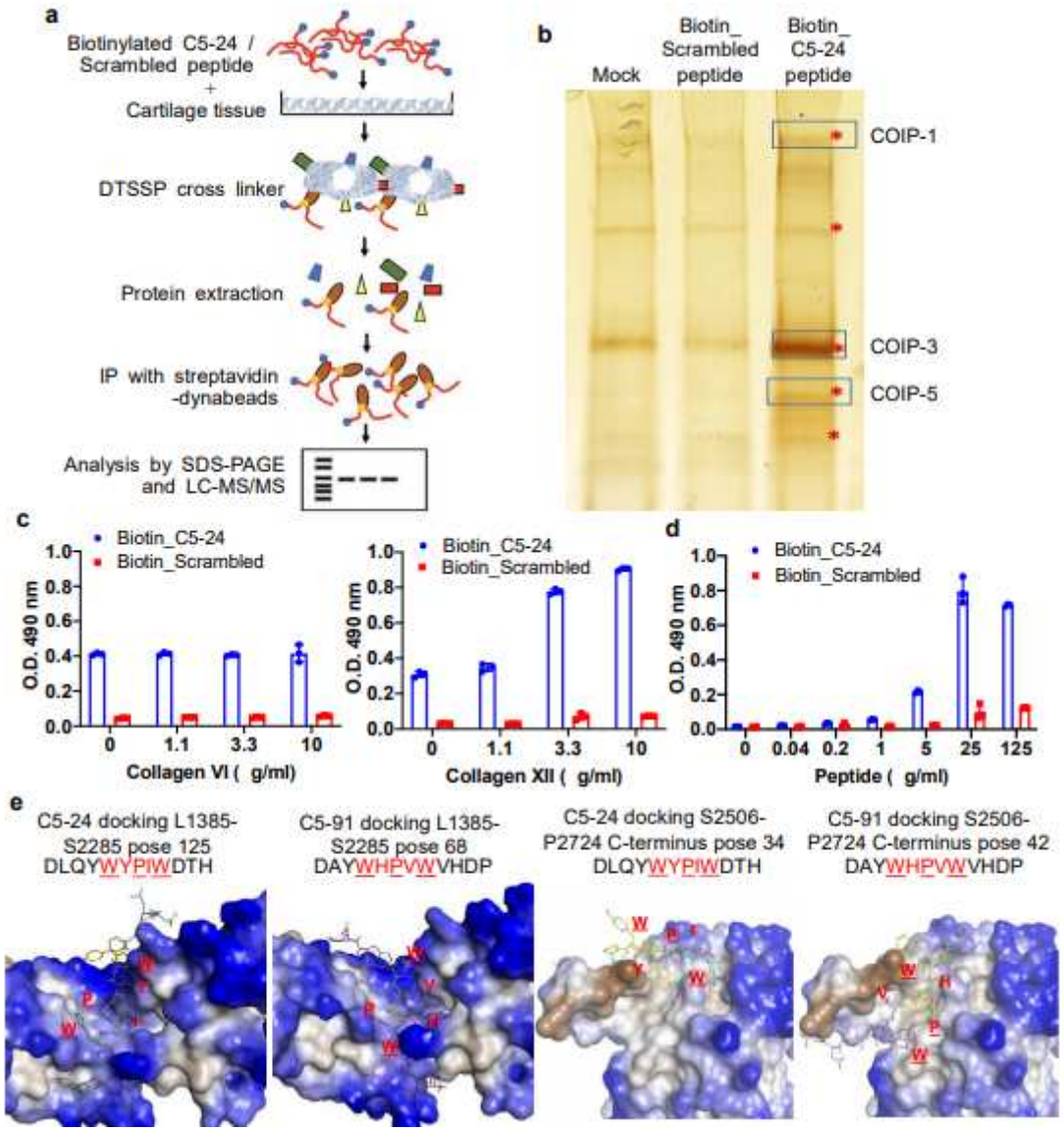

Figure 5

[Please see the manuscript file to view the figure caption.]

Supplementary Files

This is a list of supplementary files associated with this preprint. Click to download.

- Supplementaryinformation.pdf